HHS Public Access

Author manuscript

Nature. Author manuscript; available in PMC 2024 March 13.

Published in final edited form as:

Nature. 2023 July ; 619(7968): 201–208. doi:10.1038/s41586-023-06177-3.

Break induced replication orchestrates resection dependent template switch

Tianpeng Zhang[a], **Yashpal Rawal**[b], **Haoyang Jiang**[a], **Youngho Kwon**[b], **Patrick Sung**[b], **Roger A. Greenberg**[a,#]

[a]Department of Cancer Biology, Penn Center for Genome Integrity, Basser Center for BRCA, Perelman School of Medicine, University of Pennsylvania, Philadelphia, PA 19104-6160

[b]Department of Biochemistry and Structural Biology and Greehey Children's Cancer Research Institute, University of Texas Health Science Center at San Antonio, San Antonio, TX 78229

Abstract

Break induced telomere synthesis (BITS) is a RAD51 independent form of break induced replication that contributes to Alternative Lengthening of Telomeres (ALT)[1,2]. This homology directed repair mechanism utilizes a minimal replisome comprised of PCNA and DNA polymerase δ (PCNA-pol δ) to execute conservative DNA repair synthesis over many kilobases. How this long-tract homologous recombination repair synthesis responds to complex secondary DNA structures that elicit replication stress remains enigmatic[3–5]. Moreover, whether the break induced replisome orchestrates additional DNA repair events to ensure processivity is also unclear. Here, we combine synchronous double strand break induction with Proteomics of Isolated Chromatin Segments (PICh) to capture the telomeric DNA damage response proteome during BITS[1,6]. This revealed a replication stress dominated response, highlighted by repair synthesis driven DNA damage tolerance signaling through RAD18-dependent PCNA ubiquitination. Furthermore, SNM1A was identified as the major effector of PCNA-ubiquitin dependent DNA damage tolerance. SNM1A recognized the ubiquitin- modified break induced replisome at damaged telomeres, which directed its nuclease activity to promote resection. These findings reveal that break induced replication orchestrates resection dependent lesion bypass, with SNM1A nuclease activity as a critical effector of PCNA-Ub directed recombination in mammalian cells.

Break induced replication involves long-tract homology directed DNA repair synthesis that contributes to recombination dependent telomere maintenance and the repair of one-ended DNA double-strand breaks (DSBs)[1–5,7]. It differs from DNA replication in several aspects. Break induced replication is highly error prone and relies on a minimal replication complex (break induced replisome) consisting of PCNA-Pol δ for unidirectional, conservative DNA

[#]Address correspondence to Roger A. Greenberg, rogergr@pennmedicine.upenn.edu.

Contributions

R.A.G and T.Z. designed experiments. T.Z. performed all major cellular experiments with some involvement from H.J. Y.R. carried out protein purification and the nuclease assays. Y.K. and P.S. assisted in the design of the nuclease assays. T.Z. and R.A.G. wrote the manuscript with input from the other authors.

Competing interests

R.A.G. is a co-founder and scientific advisory board member of RADD Pharmaceuticals and on the scientific advisory board member of Trevarx Biomedical. Neither engagement directly relates to the substance of this study. All other authors declare no competing interests.

synthesis[1,3,4,8]. Break induced replication at telomeres and other genomic locations is associated with frequent template switches[9]. Mechanisms responsible for template switches that occur during break induced replication are undefined, as is their relationship to long-tract repair synthesis through difficult to replicate genomic structures. To address these unresolved issues, we combine complementary approaches to capture the break induced replication associated DNA damage response proteome at telomeres. Our results define break induced replication as a hybrid mechanism that couples homology directed repair synthesis with DNA damage tolerance directed recombination.

BITS triggers replication stress

Telomere specific DSB induction by the TRF1-FokI fusion protein provokes extensive homology directed repair synthesis (known as BITS) in both telomerase positive and ALT cells[1,10]. TRF1-FokI (wild-type, WT) induction results in telomere length heterogeneity and fragmentation, compared to endonuclease inactive mutant TRF1-FokI D450A (no damage control), indicating DSB associated telomere recombination that is characteristic of ALT (Extended Data Fig.1a, b). This was more pronounced in ALT dependent U2OS cells, consistent with their baseline propensity for recombination dependent telomere length heterogeneity. We used PICh[6] to acquire telomere specific DSB response proteomes introduced by TRF1-FokI (WT) in comparison to TRF1-FokI (D450A) in HeLa S3 and U2OS cell lines (Fig.1, Extended Data Fig.1c and Supplementary Table 1), representing telomerase positive and ALT cells, respectively. Telomeric chromatin factions were isolated as indicated (Fig.1a). Silver stains revealed highly purified telomere proteomes compared to scramble probe control purification (Extended Data Fig.1c). Mass spectrometry of the purified telomere proteomes demonstrated Shelterin components (TRF1, TRF2, RAP1, TIN2, TPP1, POT1)[11] were present at comparable levels regardless of damage (Fig.1c and Extended Data Table.1), whereas they were not detectable in the scramble control proteome. The conventional DNA replication machinery components (Cdc45-MCM-GINS complex, DNA Polymerases α, ε)[12] were also present at similar levels following TRF1-FokI WT or D450A induction, while the break induced replisome (RFC complex, PCNA and DNA Polymerase δ) was significantly enriched at damaged telomeres (Fig.1b, c and Extended Data Table.1) as predicted[1,3,13].

Scatterplot, heatmap and Gene Ontology analysis of the telomere damage response proteome showed a strong enrichment of DSB repair and telomere maintenance related biological processes (Fig.1b, c and Extended Data Fig.1d). Homologous recombination (HR) factors including MRE11, NBS1, RAD50 (MRN complex), BRCA1-BARD1, MMS22L-TONSL, and RAD51 became enriched after TRF1-FokI WT induction in comparison to D450A (Fig.1b). In contrast, classical non-homologous end joining (cNHEJ) factors did not (Extended Data Table.1), consistent with previous observations[10,14,15]. A predominance of ATR signaling core factors ATR, ATRIP, TopBP1 and Fanconi Anemia (FA) proteins occurred at damaged HeLa S3 and U2OS telomeres (Fig.1b, c and Extended Data Table 1). These factors were present at baseline in ALT positive U2OS cells and were further enriched upon TRF1-FokI WT induction (Fig.1b, c and Extended Data Table 1), consistent with the presence of replication stress associated damage responses at telomeres in unperturbed ALT cells[10,16,17].

A notable exception was DCLRE1A (DNA cross-link repair 1A, also known as SNM1A), a single-stranded DNA endonuclease and 5'−3' exonuclease that participates in DNA inter-strand crosslink repair in conjunction with the core FA factors (Fig.1b, c)[18,19]. SNM1A abundance increased in both HeLa S3 and U2OS cells to a much larger extent than other FA related factors, suggesting a different mode of damaged telomere localization.

PCNA-Ub recruits SNM1A to damaged telomeres

The abundance of DNA replication stress response factors at damaged telomeres stimulated us to examine the basis for this signaling mechanism (Fig.1b, c, Fig.2a and Extended Data Table 1). In response to replication fork stress, RPA in complex with ssDNA forms a platform for activation of the ATRIP- ATR kinase complex[20,21]. In accordance, western blot of PICh purified telomeres showed RPA phosphorylation (pRPA2(S33)) after TRF1-FokI WT induction (Fig.2a). Depletion of the DNA Pol δ subunit, PolD3 significantly reduced BITS associated EdU (5-ethynyl-2′-deoxyuridine) colocalization with telomeres in non-S phase cells (Extended Data Fig.1e–h)[1,22]. In this context, PolD3 depletion resulted in reduction of both RPA2 recruitment and pRPA2(S33) at telomeres (Extended Data Fig.1i–l). Together with previous reports[23,24], these data suggested BITS dependent repair synthesis promotes ATR pathway activation. Remarkably, approximately half of the PCNA present at damaged telomeres was ubiquitinated in both HeLa S3 and U2OS cells (Fig.2a). PCNA-Ub is induced by agents that introduce replication stress such as ultraviolet light (UV), hydroxyurea (HU), and methyl methanesulfonate (MMS); but not conventional DSBs from γ-irradiation or radiomimetic drugs[25–27]. PCNA-Ub associates with ubiquitin binding factors that mediate DNA damage tolerance (also known as post replicative repair) to bypass DNA lesions[28]. These results further suggest that BITS combines elements of both DSB and replication stress responses.

The E3 ubiquitin ligase RAD18 plays important roles in both DNA damage tolerance and homology-directed DNA repair[27,29]. RAD18 was significantly enriched at damaged telomeres in both U2OS and HeLa S3 cells (Fig.1b, Extended Data Fig.2a and Extended Data Table 1). Moreover, RAD18 depletion strongly reduced PCNA-Ub levels at damaged telomeres (Fig.2b). RAD18 and PCNA-Ub act as signal transducers for recombination and break induced replication[27,30], however, the downstream effectors of PCNA-Ub that mediate these processes are largely unknown. To address this question, PICh was used to isolate TRF1-FokI damaged telomere chromatin in RAD18 proficient and knock out U2OS cells (Fig.2c and Supplementary Table 2). SNM1A was the most profoundly affected factor, showing a near complete loss in the PICh purified mass spectra in RAD18 depleted U2OS cells (Fig.2c), and corresponding reductions by PICh-WB (Fig.2b). In accordance, SNM1A, together with RAD18, was one of the most enriched factors at damaged telomeres in both HeLa S3 and U2OS cells (Fig.1b, and Extended Data Fig.2a).

SNM1A, along with SNM1B (Apollo) and SNM1C (Artemis), belongs to the PSO2 (sensitive to psoralen 2)/SNM1 (sensitive to nitrogen mustard 1) family of nucleases that contain the conserved catalytic MBL (metallo-β-lactamase) and β-CASP (metallo-β-lactamase-associated CPSF Artemis SNM1/PSO2) domains[18] (Fig.2d). SNM1A appears to be the mammalian homolog of *S. cerevisiae* PSO2, possessing both single-stranded DNA

endonuclease and 5’−3’ exonuclease activities and process DNA inter-strand crosslinks *in vitro* and in yeast. Additionally, introduction of human SNM1A complemented yeast PSO2 knockouts in a manner that required its endonuclease activity[19].

SNM1A is unique among its family members by the presence of UBZ (ubiquitin-binding zinc finger) and PIP box (PCNA-interacting protein-box) motifs[31]. Both the SNM1A UBZ motif and PIP box were reported to mediate its interaction with ubiquitinated PCNA and damage induced foci formation[31]. sgRNA resistant HA-tagged SNM1A mutants cDNA were reconstituted in SNM1A knock out U2OS cells, and telomere localization was examined following TRF1-FokI induction (Fig.2d–g). SNM1A ΔUBZ and ΔPIP mutants did not localize to telomeres, whereas SNM1A ΔC and DH/AA mutants were unaffected (Fig.2f, g). These results are consistent with PCNA-Ub serving as the critical recognition element for SNM1A (Extended Data Fig.2b, c). In agreement, SNM1A and PCNA-Ub interaction by co-IP was stimulated by various agents that increase replication stress (Extended Data Fig.2d).

These observations suggest that replication stress during BITS induces RAD18-dependent PCNA-Ub to attract SNM1A. To test this hypothesis, we administered the B-family DNA polymerase (Pol α, δ and ε) inhibitor aphidicolin[32] at the time of TRF1-FokI induction in HeLa S3 cells to reduce DNA repair synthesis followed by PICh- mass spectrometry (Fig.2h, Extended Data Fig.2e and Supplementary Table 3). Aphidicolin treatment inhibited ~50% of DNA repair synthesis (Extended Data Fig.2f, g). This corresponded to reduced RAD18, PCNA-Ub and SNM1A levels at damaged telomeres as assessed by PICh- mass spectrometry and western blot (Fig.2h, i). These findings implicate BITS dependent repair synthesis in promoting the acquisition of DNA damage tolerance signaling.

RAD18 directs SNM1A dependent end resection

ALT telomeres are characterized by the presence of internal ssDNA gaps and both 5’ and 3’ ssDNA overhangs[33–35]. Telomere ssDNA further increases after TRF1-FokI induction[10]. This was evident on native southern blots of purified DNA from U2OS cells that had been treated with the 5’−3’exonuclease RecJf to remove 5’ C-rich ssDNA or with the bacterial 3’−5’ exonuclease, Exo I (*E. coli*) to remove 3’ G-rich ssDNA from telomeric overhangs (Fig.3a, b). Native FISH also revealed large increases of telomeric C-/G- rich ssDNA following TRF1-FokI induction (Extended Data Fig.3a–d). Notably, treatment with recombinant *E. coli* Exo I failed to remove much of the G-rich single stranded DNA following TRF1-FokI induction. This is consistent with the presence of recombination intermediates where G-rich ssDNA is resistant to 3’−5’ exonuclease activity (Fig.3b).

Damage induced telomeric ssDNA and RPA2 accumulation were compromised in RAD18 depleted U2OS cells (Fig.3c, d and Extended Data Fig.3e, f). Similar reductions in telomere ssDNA and RPA2 recruitment also occurred in SNM1A depleted cells (Fig.3e and Extended Data Fig.3g, h). The SNM1A UBZ, PIP box and nuclease domains were required for efficient RPA2 recruitment (Extended Data Fig.3i). SNM1A exonuclease activity on ssDNA, dsDNA and forked DNA, as well as zeocin treated plasmid DNA, was further verified by biochemical assay with purified full length SNM1A in comparison to nuclease inactivated

DH/AA mutant[36,37] (Fig.3f and Extended Data Fig.4a–e). SNM1A endonuclease activity was also confirmed with full length protein using biochemical assays on single-stranded oligonucleotide and supercoil plasmid substrates[19] (Fig. 3g and Extended Data Fig. 4f). These observations suggest RAD18 directed SNM1A nuclease activity contributes to the genesis of recombination intermediates at damaged telomeres.

In eukaryotes, DSB end resection is mediated by a series of coordinated endo- and exonuclease activities. MRE11 and CtIP initiate resection, which is propagated in a 5'−3' direction by ExoI and DNA2[38]. To determine if canonical DSB resection factors are active at damaged telomeres, we examined ssDNA formation after TRF1-FokI induction in U2OS cells with CRISPR engineered deletions in ExoI, DNA2, or MRE11 individually or in combination. Single deletions of each nuclease were performed with spCas9 or AsCas12a, whereas the simultaneous deletion of all three was achieved by combining spCas9 with the AsCas12a nuclease together with specific sgRNAs for each gene (Extended Data Fig. 5). Deletion of ExoI, DNA2 or MRE11 did not recapitulate loss of RAD18 or SNM1A with respect to ssDNA generation and RPA2 localization at telomeres (Fig. 3h and Extended Data Fig.5). ExoI loss also did not reduce accumulation of G- or C-rich ssDNA at telomeres after TRF1-FokI (Extended Data Fig. 5c). Interestingly, DNA2 loss strongly increased C-rich telomeric ssDNA regardless of TRF1-FokI induction, consistent with its role in long ssDNA flap removal during Okazaki fragment processing[39] (Extended Data Fig. 5f). In contrast, DNA2 loss reduced G-rich telomeric ssDNA specifically after TRF1-FokI induction in accordance with an involvement in 5'−3' resection at DSBs (Extended Data Fig. 5f, right panel). Nonetheless, RAD18-SNM1A clearly contributed to most of the ssDNA generation at damaged telomeres during break induced replication. These results reveal that DNA resection requirements during break induced replication differ in comparison to two-ended DSBs that are repaired by classical HR.

Template switch at damaged telomeres

We hypothesized that DNA damage tolerance pathways become active when the break induced replisome encounters telomeric secondary structures[16,34,40,41]. RAD18 mediated DNA damage tolerance involves PCNA-Ub for lesion bypass during repair synthesis[28]. This can occur by PCNA-Ub association with Y-family polymerases to execute translesion DNA synthesis (TLS)[28]. Indeed, Pol η depletion was reported to increase several ALT features, and Pol δ dependent BITS[42]. Nevertheless, loss of TLS polymerases did not impair BITS[1]. We also did not observe RAD18 dependent changes in Pol η, Pol ζ or other Y-family polymerases at damaged telomeres (Fig.1b, 2c and Extended Data Table.1), suggesting that recombination dependent effectors of PCNA-Ub may be central to damage tolerance during BITS.

RAD18 promotes recombination-mediated template switch, independent from TLS polymerases in yeast[43,44]. Template switch is a known feature of break induced replication in yeast and requires ExoI dependent resection to increase ssDNA for recombination[9,45–47]. Template switching is also reported to be frequent in telomerase deficient yeast strains that maintain telomere length by recombination dependent mechanisms[48,49]. We explored whether RAD18 was involved in telomere recombination, using native-native

two-dimensional gel electrophoresis with telomeric G-probe hybridization to visualize recombination intermediates present in the slowly migrating T-complex region (Fig.4a, b)[34]. RAD18 or SNM1A depletion strongly reduced T-complex induction by TRF1-FokI in U2OS cells (Fig.4c, d) and compromised C-circle formation at damaged telomere (Extended Data Fig.6). Chromatin orientation fluorescence in situ hybridization (CO-FISH) on metaphase chromosomes was also used to examine telomere sister chromatin exchange (T-SCE) events as an indicator of recombination mediated repair product resolution (Fig.4e). RAD18 or SNM1A depletion decreased T-SCEs in U2OS cells (Fig.4f, g). Collectively, these data suggested that RAD18 acts through SNM1A for break induced replisome driven template switch.

RAD18 and SNM1A act epistatically during BIR

RAD18 depletion reduced non-S phase telomere synthesis in either the presence or absence of TRF1-FokI induction (Fig.5a and Extended Data Fig.7a, b). Introduction of cDNA for WT RAD18 or mutants was used to determine the elements necessary for recombination dependent telomere synthesis. This demonstrated requirements for the RAD18 RING, SAP and UBZ domains (Extended Data Fig.7c, d). RAD18 E3 ligase activity and SAP domain are dispensable for canonical homologous recombination repair of DSBs, indicative that it contributes to a different form of recombination during BITS[27,29]. SNM1A depletion also impaired non-S phase telomere synthesis at TRF1-FokI damaged telomeres in U2OS cells (Fig.5b), which was restored by wild-type SNM1A, but not mutants that are defective in PCNA-Ub interaction or exonuclease activity (Extended Data Fig.7e). To pinpoint the genetic interaction between RAD18 and SNM1A, we used a dual CRISPR/Cas9 system, in which SNM1A was first knocked out with spCas9, and RAD18 was subsequently knocked out with saCas9 (Extended Data Fig.7f). In agreement with SNM1A acting downstream of RAD18, no further reduction in non-S EdU telomere localization was observed following combined depletion of RAD18 and SNM1A (Fig.5c). In contrast, knocking out MRE11, ExoI and DNA2 individually or in combination did not impair non-S phase telomere synthesis in unperturbed ALT cells or following TRF1-FokI damaged (Extended Data Fig.7g–j). We next investigated if RAD18 directed SNM1A nuclease activity during break induced replication contributes to telomere maintenance. Ectopically expressed wild type RAD18, but not mutants in the RING, SAP or UBZ domains, extended telomere length in two different ALT cell lines. RAD18 driven telomere length increases occurred in an SNM1A dependent manner (Fig.5d and Extended Data Fig.7k–m). These findings supported the hypothesis that RAD18 directs DNA damage tolerance through PCNA-Ub-SNM1A resection mediated template switching for lesion bypass during break induced replication dependent telomere maintenance.

Telomere DSBs provoke long-range unidirectional DNA repair synthesis during BITS, which resembles break induced replication at telomeres or other genomic locations[1,3,7]. Telomere secondary structures pose challenges to both conventional and break induced replication machinery[40,50]. Indeed, interstitial telomeric DNA or transcription was reported to impede break induced replication in yeast[50,51] and template switch is engaged at a high frequency to eventually resolve break induced replication in yeast[9]. Using a comprehensive analysis of the telomere damage response proteome coupled with functional analyses,

we define DNA damage tolerance by template switch to be critical for break induced replication through such impediments (Fig.5e). Damaged telomeres assemble a combination of homologous recombination and replication stress response factors in a manner that depends on DNA repair synthesis (Figs 1, 2 and Extended Data Table.1). Moreover, modification of the break induced replisome is essential to orchestrate DNA damage tolerance for continued DNA repair synthesis. Notably, different RAD18 functional domains requirements exist for DNA damage tolerance and homologous recombination repair. This, together with the requirement for PCNA-Ub, differentiates BITS from conventional DSB repair by homologous recombination, suggesting DNA damage tolerance plays a unique role in break induced replication[30] (Fig.5e). Because template switch cannot be directly visualized during these experiments, future studies will be essential to determine if other types of RAD18 and SNM1A dependent recombination also contribute to the DNA repair synthesis during BITS.

While PCNA-Ub dependent activation of TLS is well described in both human and yeast, downstream effectors of PCNA-Ub driven template switch in mammalian cells are more enigmatic. SNM1A was the most diminished factor at damaged telomeres in RAD18 depleted cells and was the functional effector of RAD18 and PCNA-Ub during BITS through DNA resection dependent template switch. SNM1A contains endonuclease and 5'−3' exonuclease activities that contribute to DNA inter-strand crosslink (ICL) repair [18,19,36,37,52]. Together these findings highlight similarities between replisome acquisition of DNA damage tolerance pathways during either replication stress or long-range DNA repair synthesis.

Template switching during BIR may occur by several rounds of invasion-synthesis-dissociation-reinvasion without end processing steps, or through other strand dissociation mechanisms that could occur in an SNM1A independent manner[9,46]. However, there are several possible requirements for resection dependent template switch during break induced replication. D-loop dissociation and interruption may occur during unstable bubble migration, especially when the break induced replisome encounters replication obstacles [7,9,50,51]. In this context, RAD18 directed PCNA-Ub- SNM1A interaction may be engaged to initiate end resection for template switch mediated strand invasion to re-establish a replication bubble using the same template strand or a different template on a telomere from another chromosome (Fig.5e). SNM1A binding to PCNA-Ub at blocking lesions would initiate endonucleolytic cleavage of the leading strand template followed by SNM1A directed 5'−3' exonuclease resection for ssDNA generation. These events would promote template switch for resumption of BITS (Fig.5e). Taken together, the break induced replisome nucleates elements of both DSB and replication stress responses to promote long tract DNA repair synthesis through complex genomic regions.

Material and Methods

Cell lines

U2OS, HeLa S3, and HEK 293T cell lines were grown in DMEM (Thermo Fisher) with 10% calf serum (Thermo Fisher) and 1% Penicillin/ Streptomycin (Thermo Fisher). VA13 and LM216J cell lines were grown in DMEM (Thermo Fisher) with 10% FBS (Bio-

Techne) and 1% Penicillin/Streptomycin (Thermo Fisher). HeLa S3 and U2OS TRF1-FokI (D450A and WT) inducible cell lines were constructed and authenticated by STR analysis (ATCC)[1]. U2OS TRF1-FokI (D450A and WT) expressing Cas9 protein were generated using lenti-SpCas9 hygro (a gift from Brett Stringer, Addgene plasmid # 104995). Cell lines were maintained in an incubator at 37°C and 5% CO_2 according to standard protocols. Cell lines were validated to be negative for mycoplasma contamination using MycoAlert Plus Mycoplasma Detection Kit (Lonza). HeLa S3 TRF1-FokI (D450A and WT) used for telomere and associated protein purification purpose (PICh) were cultured in spinner flasks. Specifically, five 15cm dishes of HeLa S3 TRF1-FokI (D450A and WT) cells were subcultured into 1 L cell culture medium in spinner flasks and agitated on magnetic stir plate at 50 rpm in a 37°C incubator with humidified atmosphere of 5% CO_2.

CRISPR mediated gene deletions

For single gene knockout, Cas9 was expressed with lenti-SpCas9 hygro (a gift from Brett Stringer, Addgene plasmid # 104995), while sgRNAs targeting candidate genes of interest were generated with lentiGuide-neo (U6-sgRNA- P2A-Neo, reconstructed from a gift from Feng Zhang, Addgene plasmid # 52963).

For SNM1A and RAD18 double knockout, SNM1A was knocked out using the spCas9 lentiCRISPRv2 hygro (a gift from Brett Stringer, Addgene plasmid #98291), while RAD18 was knocked out using all-in-one vector saCas9 system[53].

For MRE11, DNA2, ExoI triple knock out experiments, MRE11 and DNA2 were knocked out with AsCas12a system[54]. AsCas12a was expressed with AsCas12a-6xNLS-E174R/S542R (pRG232) (a gift from Junwei Shi, Addgene plasmid # 149723) in U2OS TRF1-FokI cells and then sorted with fluorescence-activated cell sorting (FACS). ExoI was subsequently knocked out with spCas9 lentiCRISPRv2 hygro (a gift from Brett Stringer, Addgene plasmid #98291). Then the sgRNA targeting genes of MRE11 and/ or DNA2 were generated with EFS-EGFP-P2A-Neo-WPRE-U6-AsCas12aDR-AsCas12aDR (pRG212) (a gift from Junwei Shi, Addgene plasmid # 149722). sgRNA sgRNA sequences were listed in Supplementary Table 4.

Cloning, lentivirus generation and transduction

The cDNA for human RAD18 (hRAD18-EGFP, Addgene plasmid # 68824), SNM1A (DCLRE1A (*Homo sapiens*) pLenti6.3/V5-DEST, HsCD00954061 from DNASU Plasmid repository) was amplified and cloned into pLenti-CMV-Neo-DEST (705–1) (a gift from Eric Campeau & Paul Kaufman, Addgene plasmid # 17392), using Gibson Assembly® Master Mix (New England Biolabs, E2611S). PCR mediated mutagenesis were done with Q5® Site-Directed Mutagenesis Kit (New England Biolabs, E0554S) to construct RAD18 and SNM1A mutations. The cloning primers are listed in Supplementary Table 4.

Plasmids together with viral packaging plasmids (psPAX2 and pMD2.G) were transfected into HEK 293T cells using Polyethylenimine (Polysciences, 23966) according to the manufacturer's protocol. Lentiviral supernatant was collected at 48hrs and 72 hrs post transfection and filtered through 0.45 μm filter and used for spin-infection of cell lines supplemented with 8 μg ml^{-1}polybrene (Sigma-Aldrich, H9268). Selection for lentivirus

infected cells were done using puromycin (2 μg ml^{-1}, Thermo Fisher, A1113803), blasticidin (5 μg ml^{-1}, Invivogen, ant-bl-1), hygromycin (100 μg ml^{-1}, Invivogen, ant-hg-1) and neomycin (400 μg ml^{-1}, Thermo Fisher, 11811031).

Proteomics of isolated chromatin segments (PICh)

Telomere and associated proteins were captured as previously described for PICh[6,55] with the following modifications. TRF1-FokI (D450A, WT) induction was performed in 1 L suspension HeLa S3 cells (~ 10^9 cells) by Doxycycline (40ng ml^{-1}, Sigma-Aldrich, D9891) addition for 18hrs and then 4-Hydroxytamoxifen (1 μM, Sigma-Aldrich, H7904) was added for another 2hrs. Related to Fig. 2h, i, 15 μM aphidicolin (Cayman Chemical Company) was added together with 4-Hydroxytamoxifen in the treated sample. For adherent U2OS cells, 40ng ml^{-1} doxycycline was added for 18hrs to 75 15cm dishes of U2OS (~ 10^9 cells) followed by 1 μM 4-Hydroxytamoxifen for another 2 hrs. Afterwards, cells were fixed with 4% formaldehyde by directly adding formaldehyde to the media for 45 minutes at room temperature with agitation. Then HeLa S3 cells were spun down and washed three times with ice-cold 1× PBS; while U2OS cells were washed three times with ice-cold 1× PBS in dishes and scrapped down in 1× PBS+ 0.05% Tween 20. The cell pellets were washed and dounced with dounce homogenizer in sucrose solution (0.3 M Sucrose, 10 mM HEPES-NaOH pH 7.9, 1% Triton-X 100, 2 mM Magnesium Acetate). Cell pellets were resuspended in Triton solution (1× PBS, 0.5% Triton X-100, 1 mM PMSF and 0.25 mg ml^{-1} RNase A (Qiagen, 19101)) and incubated overnight on a rotator at 4 °C. Cell pellets were then washed three times with ice-cold 1× PBS and two more times with lysis buffer (50mM Tris-HCl pH 8.0, 200mM NaCl, 20 mM EDTA-NaOH pH 8.0, 1% SDS). Then cell pellets were resuspended in lysis buffer supplemented with 1 mM PMSF (~2.5 folds to nuclei volume) and sonicated with BRANSON Digital Sonifier (Amplitude: 70%; Pulse cycle: 15 sec On, 45 sec Off; Total process time:7.5 min). Soluble chromatin fractions were heated at 58 °C for 5min and centrifuged at 16,000 g for 10 min at room temperature to remove insoluble pellets. Endogenous biotinylated proteins were removed with 1 mL Streptavidin Agarose (EMD Millipore, 69203–3) for 3hrs at room temperature on a rotator, and then passed through Sephacryl S-400 HR column (GE Healthcare Life Sciences, 17060901) with centrifuge at 750 g for 5 min at room temperature. Optical Density (OD260 and OD280) was measured with NanoDrop 1000 to confirm efficient RNA removal and quality of soluble chromatin. 0.1% of the sample was saved as “Input” for Western-blot. Soluble fractions were hybridized with 1500 pmol desthiobiotin labeled 2’-Fluor-RNA telomeric probes (t-Desthiobiotin TEG-Spacer18-Spacer18-UUAGGGUUAGGGUUAGGGUUAGGGUUAGGGUUAGGGUUAGGGt) or scramble probe (t-Desthiobiotin TEG-Spacer18-Spacer18-GACACCAAGCCACACGGAAAAACCAUCGGCACUCUAGCCUCGUAAAUGCAUGCCACGCc) in a thermocycler with the following protocol (25°C for 3 min; 80°C for 5 min; 37°C for 60 min; 60°C for 3 min; 37°C for 30 min; 60°C for 3 min; 37°C for 30 min; then keep at 25°C). Hybridized chromatin was pooled and centrifuged at 16,000 g for 15 min at room temperature; and then incubated with 900 μL Dynabeads™ MyOne™ Streptavidin C1 (Thermo Fisher, 65002) overnight on a rotator at room temperature. Then bound chromatin was immobilized on a magnetic stand, 0.1% was taken as the “Unbound” fraction for Western-blot assay, followed by washing five times with normal salt lysis buffer (10 mM

HEPES-NaOH pH 7.9, 100 mM NaCl, 2 mM EDTA-NaOH pH 8.0, 1 mM EGTA-NaOH pH 8.0, 0.2% SDS, 0.1% Sodium Sarkosyl) at room temperature, followed by one more wash with low salt buffer (10 mM HEPES-NaOH pH 7.9, 30 mM NaCl, 2 mM EDTA-NaOH pH 8.0, 1 mM EGTA-NaOH pH 8.0, 0.2% SDS, 0.1% Sodium Sarkosyl) at 42 °C and 1000 rpm for 5 min on a heat block. The telomere and associated proteins on beads were eluted twice with 450 μL elution buffer (75% normal salt buffer + 25% D-biotin (Invitrogen, B20656)) with following steps (37 °C and 65 °C for 30 min each). The eluted samples, as well as the "Input" and "Unbound" fractions, were then precipitated with TCA, washed with acetone, and crosslinks reversed in decrosslinking buffer (250 mM Tris-HCl pH 8.8, 2% SDS, 0.1 M 2-Mercaptoethanol). NuPAGE LDS Sample Buffer (4×, Invitrogen) was added. The de-crosslinked samples were subjected to silver staining, western-blot, and mass spectrometry (Taplin Biological Mass Spectrometry Facility at Harvard Medical School). The mass spectrometry data is shown in Supplementary Table 1–3.

Immunofluorescence - fluorescence in situ hybridization (IF-FISH)

Cells were grown on circular coverslips and fixed with 3% (w/v) formaldehyde (Sigma-Aldrich) for 15 min at room temperature. Cells were then permeabilized with 0.5% Triton X-100 in 1× PBS for 10 min on ice for most experiments, and placed in blocking buffer (1× PBS, 0.5% Tween-20 and 5% goat serum) for 1 hr at room temperature. Primary antibodies were diluted in blocking buffer and incubated in a humidified chamber overnight at 4 °C. The corresponding secondary antibodies were then incubated for 1 hr at room temperature. Coverslips were re-fixed with 3% (w/v) formaldehyde and dehydrated with ethanol (75%, 95%, 100%) and air-dried. Afterwards, coverslips were heat-denatured and hybridized with a telomeric probe (TelC-Cy3) (PNA Bio, F1002) in hybridization solution (70% deionized formamide, 0.5% Roche blocking reagent, 10mM Tris-HCl pH 7.4) for 2 hrs at 37 °C. Coverslips were then washed and mounted using Vectashield mounting medium with DAPI (Vector Labs). Images were acquired with a QImaging RETIGA-SRV camera connected to a Nikon Eclipse 80i microscope at 63× oil objective.

The following primary antibodies were used for immunofluorescence: HA.11 (1:200, 901514, Biolegend), RPA2 (Anti-RPA, clone RPA34–20) (1:200, MABE285, EMD Millipore), Phospho RPA32 (S33) (1:500, A300–246A, Bethyl Laboratories). The following secondary antibodies were used for immunofluorescence: Goat anti-Rabbit IgG (H+L) Highly Cross-Adsorbed Secondary Antibody, Alexa Fluor™ 488 (1:200, A-11034, Invitrogen); Goat anti-Mouse IgG (H+L) Highly Cross-Adsorbed Secondary Antibody, Alexa Fluor™ 488 (1:200, A-11029, Invitrogen).

Native FISH

Native FISH was performed as described with a minor modification[56]. Briefly, coverslips were fixed in 2% paraformaldehyde at room temperature for 10 min, permeabilized for 10 min in KCM buffer (0.1% Triton X-100, 10 mM Tris–HCl pH 7.5, 120 mM KCl, and 20 mM NaCl) with RNase A at 37°C for 2 hrs. Hybridization was performed in hybridization buffer containing 10 mM Tris–HCl pH 7.5, 85.6 mM KCl, 0.5% blocking reagent (Roche, 11096176001), 70% formamide, and 40 nM telomeric probe, TelC-Cy3 (PNA Bio, F1002) or TelG-Cy3 (PNA Bio, F1006) for 2 hrs at room temperature. Then coverslips were

washed, counterstained and imaged as shown above. Number of native FISH foci was quantified by Cell Profiler.

Detection of break induced telomere synthesis (BITS)

Cells were grown on coverslips. Cells were synchronized at G2/M phase using 9 μM RO-3306 (Selleck Chemicals, S7747) for 18hrs, during which TRF1-FokI was induced with 40 ng ml^{-1} Doxycycline. Then 1 μM 4-Hydroxytamoxifen was added for another 2.5 hrs together with 20 μM 5-ethynyl-2′-deoxyuridine (EdU, TCI Chemicals, E1057). Cells were fixed with 3% paraformaldehyde and permeabilized with 0.5% Triton X-100 on ice as described above, and then blocked in 3% BSA in 1× PBS for 1 hr at room temperature. Then EdU was detected with Click-iT™ Plus Alexa Fluor™ 488 Picolyl Azide Toolkit (Thermo Fisher, C10641) following manufacture protocol. Next, telomere FISH was done as described above.

BrdU Immunoprecipitation of nascent telomeres

BrdU-IP was performed as previously described[1,57]. Briefly, HeLa S3 TRF1-FokI was induced with 40 ng ml^{-1} Dox for 18 hrs, followed by 1μM 4-OHT for 2 hrs, during which 100 μM BrdU was added to label nascent DNA. Aphidicolin was added at indicated concentration if appropriate (as shown in Extended Data Figs.2e–g). Genomic DNA was then extracted from scraped cells with MasterPure Complete DNA & RNA Purification Kit (Epicenter) and sonicated using the Covaris S220 sonicator. 2 μg fragmented gDNA was diluted into 1× PBS in 50 μL, then heat-denatured at 95°C for 10 min and quenched in ice-water bath. 10% of samples were saved as “Input”. Then 2 μg anti-BrdU antibody (mouse B44, BD 347580) and 120 μL IP buffer (0.0625% Triton X-100 in PBS) was added to proceeded sample. 30 μL prewashed Protein G Magnetic Beads (Pierce) was incubated with 5μL of bridging antibody (Active Motif) for 1 h at 4°C, and added into each sample for another 1 h at 4°C. Samples were then washed with IP buffer for 3 times, followed by 1× TE buffer, and eluted twice at 65°C for 10 min in elution buffer (1% SDS in 1× TE buffer), then cleaned with ChIP DNA Clean & Concentrator Kit (Zymo Research). Samples and “Inputs” were heat-denatured at 95°C for 10 min and quenched in ice-water bath again and subjected to slot-blot on Amersham Hybond-N+ nylon membrane (GE Healthcare) for hybridization with P-32 labeled telomeric G-probe or Alu repeat-probe, respectively.

Chromosome-orientation fluorescence in situ hybridization (CO-FISH)

Chromosome-orientation fluorescence in situ hybridization (CO-FISH) was performed as presented with minor modification[58]. Cells were incubated with 7.5 μM BrdU (5-bromo-2’-deoxyuridine, Sigma-Aldrich, B5002) and 2.5 μM BrdC (5-bromo-2’-deoxycytidine hydrate, MP Biomedicals, 0210016680) for 16 hrs. And then treated with 0.1 μg ml^{-1} Colcemid (Roche, 10295892001) for ~ 2 hrs to arrest cells in metaphase. Cells were collected by trypsin, and resuspended in 0.075 M KCl pre-warmed at 37°C, and incubated for 30min at 37°C. Cells were spun down and fixed with prechilled methanol:acetic acid (3:1), spread on slides and aged overnight at room temperature. The slides were rehydrated in PBS for 5 minutes, treated with 0.5 mg ml^{-1} RNaseA (in PBS) for 15 minutes at 37°C and then stained with 0.5 μg ml^{-1} Hoechst 33258 (Thermo Fisher, H3569) for 15 minutes at room temperature. Then the slides were covered with 2× SSC and exposed to 365 nm UV

(Stratalinker 1800 UV irradiator) for 1 hr at room temperature. The nicked BrdU/BrdC labeled strands were digested with 10 U/μL of Exonuclease III (Promega, M1811) twice for 1 hr each at 37 °C. Then slides were washed with 1× PBS and dehydrated in 70%, 95% and 100% ethanol. Telomere G-/C- probes were sequentially applied at room temperature. Specifically, TelG-Alexa488 (PNA Bio, F1008) was applied in hybridization buffer (10% Dextran Sulfate, 50% deionized Formamide, 2× SSC) for 90 min. Slides were washed with Wash Buffer-1 (10 mM Tris-HCl pH 7.5, 1 mg ml^{-1} BSA, 70% Formamide). Second probe TelC-Cy3 (PNA Bio, F1002) was applied hybridization buffer for 90 min. Then, slides were washed twice in Wash Buffer-1 (10 mM Tris-HCl pH 7.5, 1 mg ml^{-1} BSA, 70% Formamide), twice in 2× SSC, at 37 °C for 10 min each, and three times in Wash Buffer-2 (TBST, 100 mM Tris-HCl pH 7.5, 150 mM NaCl, 0.08% Tween-20) for 5 min at room temperature. Finally, slides were dehydrated with ethanol series 70%, 95% and 100%; air-dried and mounted using Vectashield mounting medium with DAPI (Vector Labs).

Immunoprecipitation

Immunoprecipitation was performed as previously described with minor modification[1]. HA-SNM1A or mutants were reconstituted in SNM1A KO cells in U2OS TRF1-FokI cells, or overexpressed in HeLa S3 TRF1-FokI cells, respectively. Cells were first collected and washed in PBS, then resuspended in hypotonic buffer (10 mM HEPES pH 7.4, 10 mM KCl, 0.05% NP-40, and 1× cOmplete protein inhibitor cocktail (Roche)) on ice for 20 min and subsequently spun down at 14,000 rpm at 4 °C. Nuclei was collected and washed with hypotonic buffer again and spun down at 14,000 rpm at 4 °C. Then nuclei were lysed in IP buffer (100 mM NaCl, 0.2% NP-40, 1 mM $MgCl_2$, 10% Glycerol, 5 mM NaF, 50 mM Tris-HCl pH 7.5, 50 U ml^{-1} Benzonase (Sigma Aldrich) and 1× cOmplete protein inhibitor cocktail (Roche)) for 1 hr on ice, and subsequently spun down at 14,000 rpm at 4 °C. After collecting the supernatant, NaCl and EDTA concentration were adjusted to 150 mM and 2 mM, respectively. Protein concentrations were measured and adjusted, while 5% of lysates were saved as “Input”. 500 μg protein lysates were then incubated with 5 μL Ezview™ Red Anti-HA Affinity Gel (Sigma Aldrich) on rotator overnight at 4 °C. The beads were washed five times with IP buffer, followed by protein elution with 2× NuPAGE LDS Sample Buffer (Invitrogen) with 5% β-ME for 5 min at 95 °C. Samples were then analyzed by western blot.

SDS-PAGE and Western blot

Cell pellets were lysed with RIPA buffer supplemented with cOmplete protein inhibitor cocktail (Roche) on ice. Supernatants were taken after centrifugation. Protein concentration was then measured with Protein Assay Dye Reagent (Bio-Rad, 5000006). Proteins were separated by SDS-PAGE using 4–12% Bis–Tris gel (Invitrogen) and transferred onto an Amersham Protran 0.2 μm nitrocellulose membrane (Amersham, 10600004) using standard procedures. Membranes were blocked with 5% milk and sequentially incubated with primary antibodies (listed below and Supplementary Table 4) overnight at 4 °C and corresponding secondary antibodies (ECL Anti-Mouse IgG, Horseradish Peroxidase linked whole antibody (from sheep) (WB:1:2000, Sigma-Aldrich/GE, NA931) or ECL Anti-Rabbit IgG, Horseradish Peroxidase linked whole antibody (from (from donkey) (WB:1:2000, Sigma-Aldrich/GE, NA934), and eventually developed using Western Lightning Plus-ECL (Perkins Elmer, NEL105001EA).

The following primary antibodies were used for western blot: ATR (1:1000, sc-515173, Santa Cruz), ATRIP (1:1000, 2737T, Cell Signaling Technology), Phospho RPA32 (S33) (1:1000, A300–246A, Bethyl Laboratories), PCNA (1:1000, 13110S, Cell Signaling Technology), Ubiquityl PCNA (Lys164) (1:1000, 13439S, Cell Signaling Technology), PolD3 (1:1000, H00010714-M01, Abnova), FANCD2 (1:1000, sc-20022, Santa Cruz), Mre11 [12D7] (1:1000, GTX70212, GeneTex), RAD51 (1:1000, 70–001, BioAcademia), KU70 (1:1000, A302–624A, Bethyl Laboratories), XRCC4 (1:1000, sc-365055, Santa Cruz), TRF2 (1:1000, NB110–57130, Novus Biologicals), GAPDH (1:1000, 2118S, Cell Signaling Technology), Monoclonal ANTI-FLAG® M2 antibody (1:1000, F1804, Mouse), RAD18 (1:1000, 9040S, Cell Signaling Technology), SNM1A (1:1000, A303–747A, Bethyl Laboratories), mCherry (1:1000, ab183628, Abcam), H2A (1:1000, 07–146, EMD Millipore), ExoI (1:1000, A302–640A-T, Bethyl Laboratories), α-Tubulin (1:200, 12G10, Developmental Studies Hybridoma Bank), HA.11 (1:1000, 901514, Biolegend), Phospho ATR (Thr1989) (1:1000, 58014S, Cell Signaling Technology), DNA2 (1:1000, ab96488, Abcam), GFP (D5.1) (1:1000, 2956S, Cell Signaling Technology).

Telomere restriction fragment (TRF) Analysis

Telomere restriction fragment (TRF) analysis was used to measure telomere length as described[1,56]. Genomic DNA was extracted using DNeasy Blood & Tissue Kit (Qiagen, 69506), and measured (Qubit 3.0 Fluorometer, Thermo Fisher Scientific). 5 μg genomic DNA was digested with Hinf I (New England Biolabs, R0155S) and Rsa I (New England Biolabs, R0167L).

For constant-field gel electrophoresis, the digested DNA was separated using the Owl™ A5 Large Gel System (Thermo Fisher) with conventional 0.7% agarose gel in 1× TAE buffer at 2V/cm for 20h in cold room.

For pulsed-field gel electrophoresis, the digested DNA was separated using the CHEF-DRII system (Bio-Rad). Samples were loaded in 1% pulse field (PFGE) certified agarose (1620137, BioRad) in 0.5× TBE buffer using following parameter: 4 V/cm; initial switch time 5 sec, final switch time 5 sec, for 20 hrs or 24 hrs at 14 °C.

The gel was dried for 4hrs at 42 °C, and stained with Ethidium Bromide (Sigma-Aldrich, 2375), and subjected to denatured in-gel hybridization as shown below.

Neutral-neutral two-dimensional gel electrophoresis

Neutral-neutral two-dimensional gel electrophoresis was performed as previously described[34,56]. Briefly, gDNA was extracted and digested as described for TRF analysis. Restriction enzyme digested gDNA were first resolved with 0.4% agarose gel in 1× TBE at 1V/cm at room temperature for 9 hrs (6 samples). The lanes were then cut and soaked in 1× TBE with 0.3 μg ml^{-1} Ethidium Bromide (EB), then casted into 1% agarose gel containing EB in 1× TBE. Second dimensional gel electrophoresis was operated at 3 V/cm for 6hrs in the cold room. The gel was dried for 4 hrs at 42 °C and subjected to native and denatured in-gel hybridization as shown below sequentially.

Native and denatured in-gel hybridization

For native hybridization, the dried gel was first prehybridized with Denhart's hybridization buffer, then hybridized overnight at 42°C with ^{32}P-labeled C- or G- telomeric probe prepared as shown before[59]. The hybridized gel was then washed 3 times with 2× SSC and 0.5% SDS and 3 times with 2× SSC + 0.1% SDS, then exposed to PhosphorImager screen (GE Healthcare) and scanned on STORM 860 imager with ImageQuant (Molecular Dynamics). For denatured hybridization, gel was first denatured with 0.5 M NaOH + 1.5 M NaCl; neutralized with 0.5 M Tris–HCl pH 8.0 + 1.5 M NaCl for half hour each; and then prehybridized and hybridized as native hybridization.

C-circle assay

C-circle assay was performed as before[60]. Genomic DNA was digested with Hinf I (New England Biolabs, R0155S) and Rsa I (New England Biolabs, R0167L). 30 ng of digested DNA in 10 μL was combined with 10 μL of 2× C-circle amplification master buffer (0.4mg ml^{-1} BSA, 0.2% Tween 20, 2mM dATP, dGTP and dTTP each, 2× Φ29 Buffer and 15 U Φ29 DNA polymerase (Thermo Fisher)) for 8h at 30°C, and then subjected to slot-blot and hybridization with C-probe. Then samples were incubated for 8 h at 30 °C, followed by 20 min at 65 °C. Samples were then diluted in 2× SSC buffer and slot-blotted onto Amersham Hybond-N+ nylon membrane (GE Healthcare). Membrane was ultraviolet crosslinked and then hybridized with ^{32}P-labeled C-probe in PerfectHyb Plus Hybridization Buffer (Sigma) overnight at 42 °C. Then, the membrane was washed twice in 2× SSC buffer + 0.1% SDS, exposed, scanned, and analyzed as shown above.

SNM1A expression and purification

Wild-type and mutant (DH/AA) SNM1A were expressed in Hi5 insect cells using baculoviruses for 48 hrs and purified by a combination of conventional chromatographic fractionation. For protein purification, crude cell lysates were prepared from a 40 g cell pellet (harvested from 5L of insect cell culture) by sonication in 100 ml T buffer (25 mM Tris-HCl, pH 7.5, 10% glycerol, 0.5 mM EDTA, 1mM DTT, 0.5% IGEPAL, 20 mM imidazole, 1 mM PMSF and protease inhibitors) containing 100 mM KCl, followed by centrifugation at 100,000 g for 60 min. The clarified lysate was loaded onto a 5-ml column of Hitrap SP FF and fractionated with a 50 ml, 100–600 mM KCl gradient in T buffer. Fractions containing SNM1A protein were collected and diluted with T buffer to adjust salt concentration to 100 mM and fractionated in a 5-ml HiTrap Heparin column with a 50 ml, 100–600 mM KCl gradient in T buffer. For further purification, fractions containing SNM1A were diluted to adjust salt concentration to 100 mM and fractionated first through a 1-ml HiTrap SP HP column and then through a 1-ml HiTrap Heparin 1 ml column with a 45 ml 150–600 mM KCl gradient in T buffer. Peak fractions were pooled and concentrated to 0.4 ml in an Amicon 30 concentrator and then subject to size exclusion chromatography in a Superose 6 Increase 10/300 GL column in T buffer containing 400 mM KCl. The peak fractions were concentrated and 2-μl aliquots were snap frozen in liquid nitrogen and stored at −80°C.

SNM1A nuclease activity assay

SNM1A exonuclease and endonuclease activities were tested at 37°C in 10 μl reaction buffer containing 20 mM Na-HEPES pH 7.5, 2 mM ATP, 0.1 mM DTT, 100 mg/mL BSA, 0.05% Triton X-100. For testing exonuclease activity, the indicated amount of SNM1A or $SNM1A^{DH/AA}$ was incubated with 5 nM of 5' ^{32}P-labeled 80-nt ssDNA (P1 oligonucleotide, 5'-TTATATCCTTTACTTTGAATTCTATGTTTAACCTTTTACTTATTTTGTATTAGCCGGATCCTTATTTCAATTATGTTCAT), 80-bp dsDNA (P1 and P2 oligonucleotides, 5'-ATGAACATAATTGAAATAAGGATCCGGCTAATACAAAATAAGTAAAAGGTTAAACATAGAATTCAAAGTAAAGGATATAA) or fork DNA (P1 and P5 oligonucleotides, AATAAATATAGGAAATGAAATAAAAGAGACATAAATAAGAAGTAAAAGGTTAAACATAGAATTCAAAGTAAAGGATATAA) with a 41-bp duplex region and 39 nucleotides overhangs for 30 min in presence of 10 mM $MgCl_2$ and/or 10 mM $MnCl_2$. Then, SDS (0.2%) and proteinase K (0.25 mg mL^{-1}) were added, followed by a 10-min incubation to deproteinize the reaction mixtures. Nuclease products were resolved in 10% polyacrylamide gels in TBE buffer (45 mM Tris-borate and 1 mM EDTA). Gels were dried and subjected to phosphorimaging analysis with Amersham Typhoon phosphorimager (Cytiva) and the ImageQuant software (Cytiva). To test for endonuclease activity, SNM1A or $SNM1A^{DH/AA}$ was incubated with 5 nM of 5' Cy5-labeled 80-nt ssDNA (5'-Cy5//iSp9/TTATGTTCATTTTTTATATCCTTTACTTTATTTTCTCTGTTTATTCATTTACTTATTTTGTATTATCCTTATCTTATTTA)_for 30 min and reactions mixtures were deproteinized and analyzed, as above. Gels were directly analysed in a BioRad ChemiDoc MP imaging system.

SNM1A nuclease activity was tested using ϕX174 replicative form DNA by analyzing either nicking of supercoiled DNA or digestion of DNA pretreated with Zeocin to induce DNA strand breaks as described[61]. For Zeocin treatment, 4 μg phiX174 supercoiled DNA was incubated with 0.5 mg ml^{-1} Zeocin (R25001, Thermo Fisher) for 20 min at 37°C in 50 μL buffer containing 12.5 mM Tris-HCl pH 8.0, 300 mM sucrose, 0.02% TritonX-100, 1.25 mM EDTA, 5 mM $MgCl_2$, 1% BSA, 100 mM ferrous ammonium sulphate, and 7.5 mM β-mercaptoethanol, and then reaction was cleaned up by Wizard SV Gel and PCR Clean-Up system (Promega, A9281) column purification. The indicated amount of SNM1A or $SNM1A^{DH/AA}$ was incubated with 40 ng of ϕX174 supercoiled DNA or 50 ng of Zeocin treated ϕX174 DNA in a 10 μL reaction with 10 mM $MgCl_2$. After deproteinization, reaction mixtures were resolved in a 1% agarose gel in TAE buffer (40 mM Tris base, 20 mM acetic acid and 1 mM EDTA). DNA species were stained with ethidium bromide and then analyzed in the ChemiDoc MP imaging system.

Statistics and reproducibility

All statistical analyses were performed using GraphPad Prism 9 software. All data were assembled into figures with Adobe Illustrator 2023. Significance was calculated by the unpaired two-tailed Student's *t*-test. *p* values are shown in the figures. All source data, uncropped images, and brief instructions about data organization are provided. Bar graphs, related to in gel hybridization and nuclease activity assay, showing mean ± SEM of independent experimental results, where the replicates number are shown in figure legends (Figs. 3a–b, 3d–g, and Extended Data Figs. 2g, 4b–f, 5c, 5f, 6a–b). The mean of "Relative

intensity of T-complex" of southern blot of neutral-neutral 2D gel electrophoresis in Figs. 4b–d from 3 or 5 independent experiments were shown below gel. The microscopy related images, including IF-FISH, EdU-FISH colocalization, native-FISH, CO-FISH, were randomly taken, while the representative images are shown in figures (Figs.2f, 4e and Extended Data Figs.1g, 1i, 1k, 3a, 3c. The quantification analysis in Figs. 2g, 3h, 5a–c and Extended Data Figs. 1h, 1j, 1l, 3b, 3d, 3f, 3h, 3i, 5b, 5e, 5h, 7b, 7d–e, 7g–j are the aggregate of three biological replicates, whereas the CO-FISH experiments were performed twice in Figs. 4f–g). The error bars show the mean ± SEM in the scatter plots. Cell numbers per condition are provided in the figure legends. Scatter plot, heatmap, and GO term analysis, in Figs. 1b–c, 2c, 2h and Extended Data Fig. 1d, for PICh-MS results are derived from an average of two independent experiments (peptide number of the experiments are provided in Supplementary Table 1–3). Western blots (WB) checking protein expression level after overexpression and/or CRISPR knockout were performed at least three times in Figs. 2e and Extended Data Figs. 1a, 1e, 3e, 3g, 5a, 5d, 5g, 5j, 7a, 7c, 7f, 7k–l. Three independent immunoprecipitation experiments and the western blot experiments were done (Extended Data Figs. 2a–d). Two independent PICh-Silver staining (Extended Data Fig. 1c) and PICh-WB were performed in (Figs. 2a, 2b, 2i and Extended Data Fig. 2a). Fig. 2a is aggregated from different membranes with same PICh experiment samples, where the corresponding uncropped raw images are provided. Coomassie blue staining and Western-blot in Extended Data Fig.4a were done step-by-step during purification, only final validation are shown. TRF experiments were done at least twice in Figs. 5d and Extended Data Figs. 1b, 7m). No statistical methods were used to predetermine sample size. The experiments were not randomized, and the investigators were not blinded to allocation during experiments and outcome assessment.

Extended Data

		HeLa S3				U2OS			
		Exp #1		Exp #2		Exp #1		Exp #2	
	Gene	D450A	WT	D450A	WT	D450A	WT	D450A	WT
Shelterin	TERF2	193	304	140	175	317	245	259	183
	TERF1	433	306	217	185	368	224	264	205
	TINF2	95	116	90	115	125	107	151	108
	TERF2IP	116	203	125	177	235	222	228	158
	POT1	95	109	74	95	84	58	49	45
	TPP1	24	33	21	43	28	23	28	23
	ATM	1	7	0	13	9	9	2	7
	MDC1	0	0	0	0	18	18	8	6
MRN Complex	MRE11	56	140	38	99	68	118	39	121
	RAD50	96	246	46	179	138	208	85	239
	NBN	32	86	30	71	48	84	33	88
Homologous Recombination	BRCA1	0	6	0	3	10	18	1	3
	BARD1	0	1	0	0	1	5	1	8
	MMS22L	1	20	1	9	1	16	3	34
	TONSL	12	30	6	13	10	27	8	54
	RAD51	0	3	0	4	0	2	1	4
Non-homologous End-Joining	PRKDC	191	286	108	183	192	172	123	126
	XRCC6	120	130	64	95	128	117	111	133
	XRCC5	67	98	51	77	115	97	88	110
	TP53BP1	0	0	3	11	9	15	1	5
	RIF1	0	10	0	9	19	19	7	0
	XRCC4	0	0	1	2	0	2	1	5
	Lig4	0	0	0	0	0	0	0	0
	DCLRE1C	0	0	0	0	0	0	0	0
	SFPQ	20	28	10	12	40	32	22	25
	NONO	19	17	21	21	26	35	30	24
	XLF/NHEJ1	0	0	0	0	0	0	0	0
	SMCHD1	59	39	30	22	66	43	65	41
Break induced telomere synthesis	RFC1	5	36	4	25	22	46	15	86
	RFC2	5	23	7	19	12	20	9	31
	RFC3	5	13	2	14	5	14	1	10
	RFC4	14	21	8	17	11	18	5	37
	RFC5	5	19	8	15	9	13	5	22
	PCNA	26	141	23	157	27	94	25	130
	POLD1	30	62	17	39	13	17	19	33
	POLD2	10	21	10	16	8	9	5	8
	POLD3	4	12	3	9	3	4	3	5
Conventional Replisome	CDC45	0	0	0	0	2	2	0	2
	MCM2	62	70	48	61	102	85	89	63
	MCM3	57	73	33	52	124	95	101	58
	MCM4	33	64	38	57	83	57	87	61
	MCM5	31	52	29	43	69	58	74	46
	MCM6	46	76	28	34	77	67	43	31
	MCM7	75	77	48	55	126	99	92	66
	GINS1	2	3	2	3	5	4	1	2
	GINS2	0	4	2	2	4	3	0	2
	GINS3	1	3	0	2	5	5	0	1
	GINS4	3	5	3	5	9	4	6	2
	POLA1	0	2	3	14	17	8	9	9
	POLA2	0	5	0	0	3	1	0	0
	POLE	0	1	1	3	17	15	11	10
	POLE3	1	1	3	3	3	4	0	0
	POLE4	0	0	0	2	1	0	0	0
	POLB	2	6	2	8	2	8	0	9
	POLH	0	0	0	0	1	0	0	0
Alternative End Joining	PARP1	81	95	41	53	77	70	63	52
	PARP2	1	2	0	0	0	0	0	1
	LIG1	0	54	1	26	0	20	8	31
	LIG3	13	54	10	41	8	62	9	76
	XRCC1	7	20	11	17	8	31	5	30
	ERCC1	8	8	8	11	21	19	18	16
	ERCC4	36	46	31	42	66	88	60	49
	FEN1	27	41	19	42	35	33	25	43
	APEX1	4	11	11	11	26	22	5	9
ATR signaling pathway	ATR	0	66	0	37	28	56	20	38
	ATRIP	0	7	0	5	2	16	1	6
	TOPBP1	0	39	2	25	24	44	14	36
	RBBP8	0	1	0	4	0	5	2	8
	RPA1	96	149	77	128	107	98	119	114
	RPA2	21	26	26	37	25	28	29	22
	RPA3	9	8	5	9	5	4	6	4
	RAD9A	10	10	3	9	3	8	5	10
	RAD1	6	11	4	15	6	6	3	2
	HUS1	1	3	2	3	4	4	3	2
Fanconi Anemia	FANCD2	1	56	0	17	45	53	23	32
	FANCI	6	66	2	26	61	72	25	39
Exonuclease	EXO1	0	0	0	0	0	0	0	0
	DCLRE1A	0	56	0	35	4	35	1	31
	DCLRE1B	33	49	8	21	69	50	47	25
DNA damage tolerance	Rad18	2	14	1	10	12	20	2	21
	HLTF	7	23	10	19	0	1	0	0
	SHPRH	0	0	0	0	0	0	0	0
	ZRANB3	0	0	0	0	0	0	0	0
Mismatch repair	MSH2	50	116	40	91	39	91	43	162
	MSH3	2	24	0	16	2	6	0	5
	MSH6	47	146	31	81	66	120	56	159
	MLH1	2	1	0	2	6	2	5	3

Extended Data Figure 1-related to Figure 1. Break induced telomere synthesis triggers replication stress

a. TRF1-FokI (D450A, WT) was induced with doxycycline for 18 hrs, followed by 4-OHT for 2 hrs. Whole cell extracts were separated with SDS-PAGE and blotted with Flag antibody (for Flag tagged TRF1-FokI), and GAPDH (loading control) antibodies.

b. Telomere restriction fragment (TRF) analysis of telomere length from HeLa S3 and U2OS cells induced with TRF1-FokI (D450A, WT) as shown in (a), respectively, using ^{32}P-labeled telomeric C-probe under denaturing condition.

c. Silver staining of telomere chromatin bound fractions enriched by PICh with telomeric probe (Telo) or scramble probe (SCR) in HeLa S3 (left) or U2OS (right) induced with TRF1-FokI (D450A, WT) for 2 hrs.

d. Gene ontology (GO) terms significantly enriched at damaged telomeres in both HeLa S3 and U2OS. Fold change of (WT+1)/(D450A+1) of total peptide number in both HeLa S3 and U2OS cells were calculated. Greater than two-fold increases in peptide number in both cell lines was analyzed.

e. Western blot showing PolD3 depletion, with sgRNA targeting Rosa (sgCtrl) or PolD3 (sgPolD3), from U2OS cells induced with TRF1-FokI for 2 hrs. Whole cell extracts were separated with SDS-PAGE and blotted with mCherry (for mCherry tagged TRF1-FokI), PolD3, and GAPDH (loading control) antibodies.

f. Experimental procedure of telomere synthesis in G2/M synchronized U2OS cells +/− TRF1-FokI induction.

g. Representative images of EdU (Green) and telomeres (Telo, Red) in S phase and non-S phase U2OS cells that were arrested in G2 by RO-3306 and induced with TRF1-FokI for 2.5 hrs.

h. Quantification of (g) for EdU colocalization with telomeres in PolD3 knocked out (sgPolD3) or control (sgCtrl) U2OS cells following TRF1-FokI induction for 2.5 hrs in G2 phase. Data represent the mean ± SEM of three independent experiments (n = 184, 222, 170, 203 (left to right)). Statistical analyses are done with unpaired two-tailed student's *t*-test. *p* values are shown.

i. Representative IF-FISH images of RPA2 (Green) colocalization with telomere (Telo, Red) in U2OS cells induced with/ without TRF1-FokI for 2 hrs.

j. Quantification of (i) for number of RPA2 and telomere foci colocalization events in U2OS cells induced with TRF1-FokI for 2 hrs with sgRNA targeting Rosa (sgCtrl) or PolD3 (sgPolD3). Data represent the mean ± SEM of three independent experiments (n = 322, 286, 287, 270 (left to right)). Statistical analyses are done with unpaired two-tailed student's *t*-test. *p* values are shown.

k. Representative IF-FISH images of pRPA2(S33) (Green) colocalization with telomeres (Telo, Red) in U2OS cells induced with TRF1-FokI for 2 hrs.

l. Quantification of (k) for number of pRPA2(S33) and telomere foci colocalization events in U2OS cells +/− TRF1-FokI induction for 2 hrs in cells with sgRNA targeting Rosa (sgCtrl) or PolD3 (sgPolD3). Data represent the mean ± SEM of three independent experiments (n = 306, 392, 371, 350 (left to right)). Statistical analyses were performed using an unpaired two-tailed student's *t*-test. *p* values are shown.

The uncropped gel images are provided in Supplementary Fig. 1.

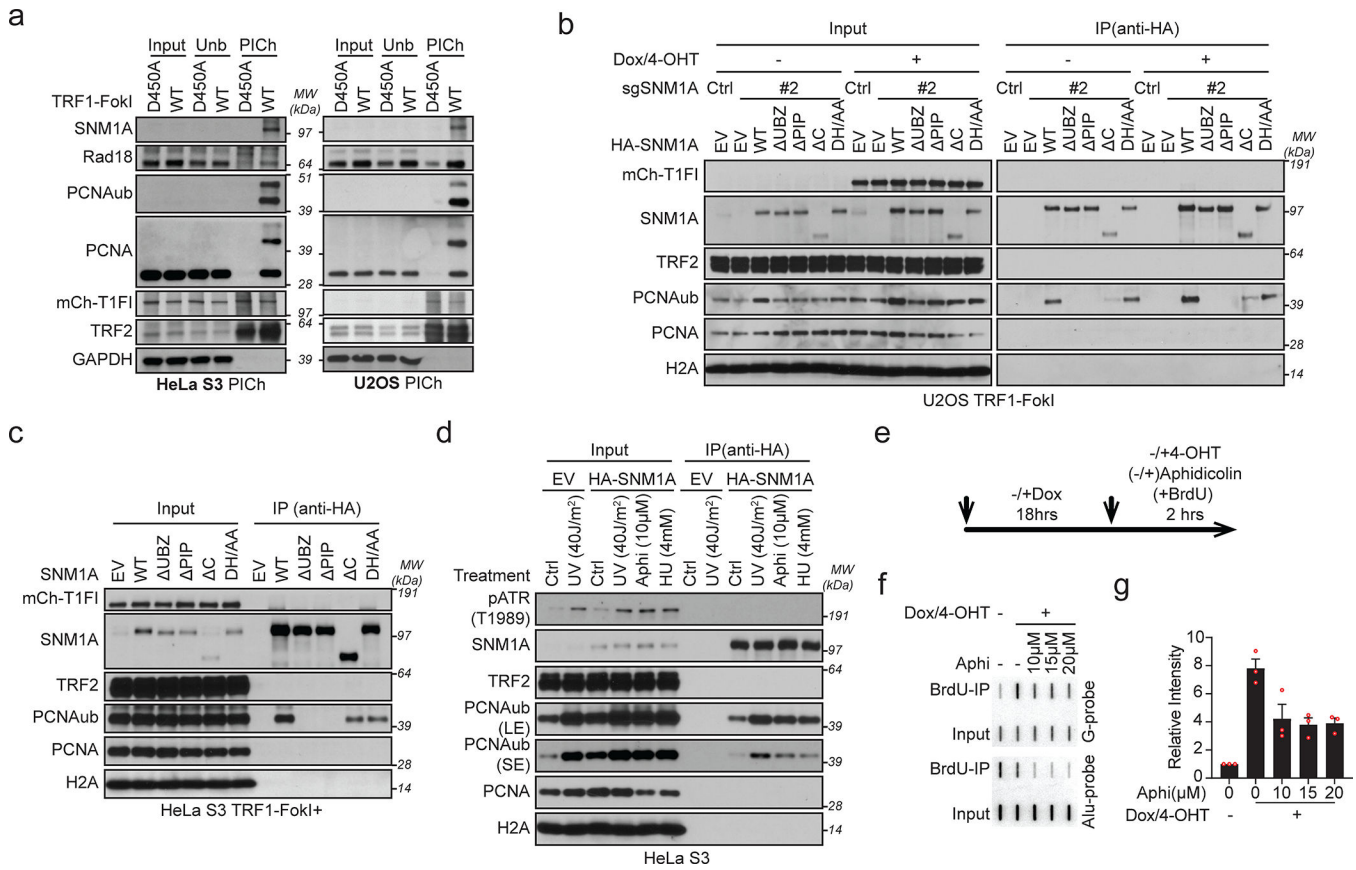

Extended Data Figure 2-related to Figure 2. BITS triggers RAD18 mediated PCNA-Ub and SNM1A recruitment at damaged telomeres

a. PICh-WB for telomere associated RAD18, SNM1A, PCNA and PCNA-Ub (Ubiquitylated PCNA (Lys164)) in HeLa S3 and U2OS induced with TRF1-FokI (D450A and WT), respectively. GAPDH, TRF2 and mCherry (mCherry tagged TRF1-FokI) were blotted as experimental controls.

b-c. Nuclear extracts from U2OS cells or HeLa S3 stably expressing SNM1A (or mutants) following induction with TRF1-FokI for 2 hrs were subjected to immunoprecipitation (IP) with anti-HA antibody. Input and IP samples were separated with SDS-PAGE and blotted with mCherry (for mCherry tagged TRF1-FokI), SNM1A, TRF2, ubiquitinated PCNA, PCNA and H2A (loading control) antibodies.

d. Nuclear extracts from HeLa S3 stably expressing SNM1A (or mutants) after treatment with replication stress agents were subjected to immunoprecipitation (IP) with anti-HA antibody. Input and IP samples were separated with SDS-PAGE and blotted with pATR (T1989), SNM1A, TRF2, ubiquitinated PCNA (Ubiquityl PCNA (Lys164)), PCNA and H2A (loading control) antibodies. “LE”: long exposure; “SE”: short exposure.

e. Experimental procedure for BrdU-IP (for (**f**)) or PICh (Fig.2h, i) in HeLa S3 cells induced with TRF1-FokI with aphidicolin at the indicated concentrations.

f. BrdU pulldown slot blot for telomere (or Alu) content using ^{32}P-labeled telomeric G-probe or Alu probe, from HeLa S3 cells induced with TRF1-FokI for 2 hrs in presence of aphidicolin (Aphi).

g. Quantification of (**f**). Relative abundance of telomere content enriched by BrdU pulldown are normalized to the uninduced sample. Data represent the mean ± SEM of three independent experiments.

The uncropped gel and dot blot images are provided in Supplementary Fig. 1.

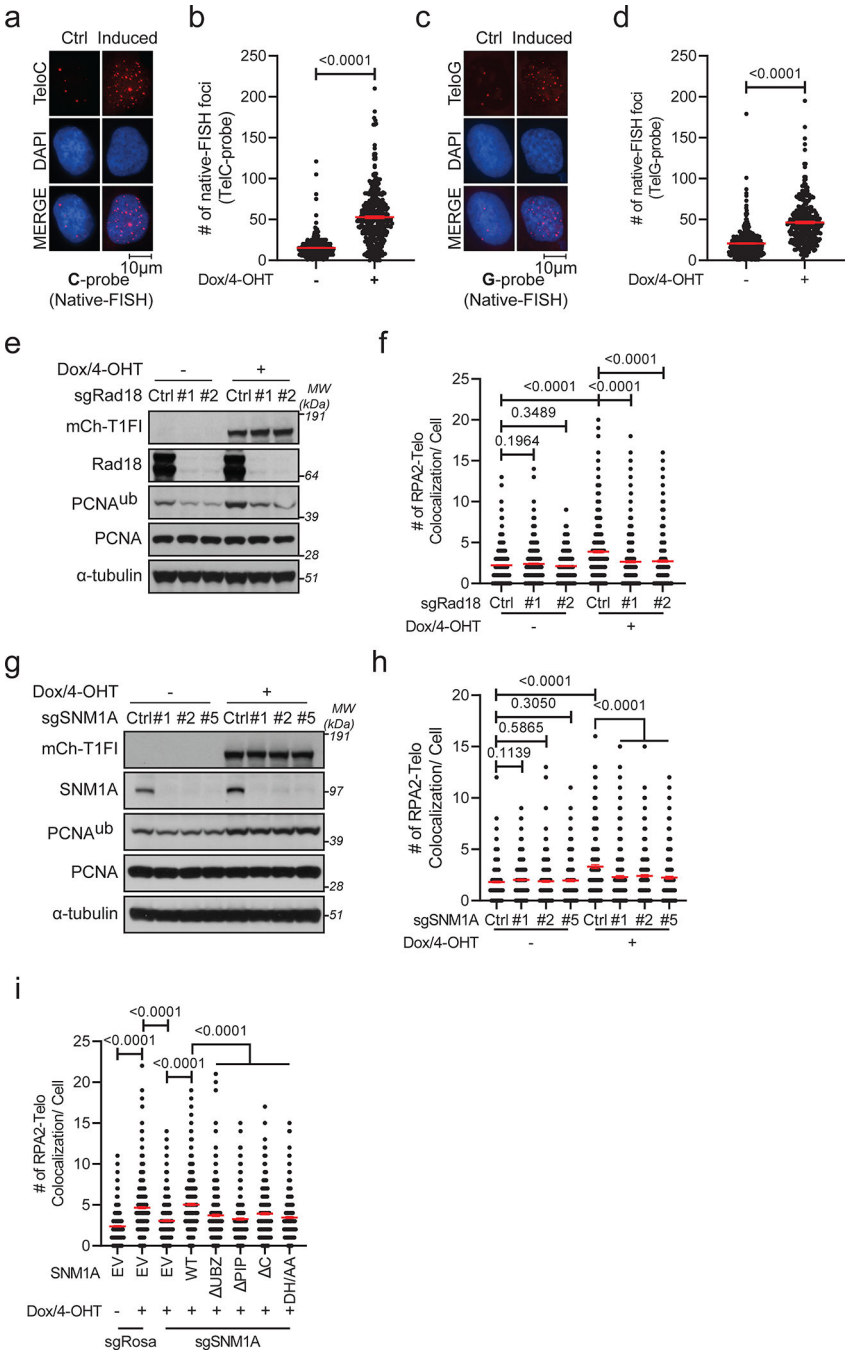

Extended Data Figure 3-related to Figure 3. RAD18 and SNM1A are required for ssDNA generation at damaged telomeres

a-d. Representative images (a) and (c) and quantification (b) and (d) of native-FISH by telomeric C-probe (TelC-Cy3, Red) and G-probe (TelG-Cy3, Red) in U2OS cells

induced with TRF1-FokI for 2 hrs. Data represents the mean ± SEM of three independent experiments (n = 354, 343 in (b) and n = 335, 288 in (d). Statistical analyses were performed using an unpaired two-tailed student's *t*-test. *p* values are shown.

e. Western blot of RAD18 from U2OS cells induced with TRF1-FokI for 2 hrs. Rad18 was knocked out with sgRNAs (#1, #2).

f. Quantification of RPA2 and telomere foci colocalization events in U2OS cells induced with TRF1-FokI for 2 hrs as indicated. Data represent the mean ± SEM of three independent experiments (n = 638, 553, 594, 547, 522, 532 (left to right)). Statistical were performed using an unpaired two-tailed student's *t*-test. *p* values are shown.

g. Western blot of SNM1A from U2OS cells following induction with TRF1-FokI for 2 hrs in cells with sgRNA targeting Rosa (sgCtrl) or SNM1A (sgSNM1A #1, #2, #5).

h. Quantification of number of RPA2 and telomere foci colocalization events in U2OS cells following induction with TRF1-FokI for 2 hrs as indicated. Data represent the mean ± SEM of three independent experiments (n = 354, 350, 286, 282, 281, 331, 339, 270 (left to right)). Statistical analyses were performed using an unpaired two-tailed student's *t*-test. *p* values are shown.

i. Quantification of number of RPA2 and telomere foci colocalization events in SNM1A knocked out U2OS cells reconstituted with sgRNA resistant SNM1A or mutants following TRF1-FokI induction for 2 hrs. Data represent the mean ± SEM of three independent experiments (n = 495, 536, 442, 390, 416, 368, 483, 396 (left to right)). Statistical analyses were performed using an unpaired two-tailed student's *t*-test. *p* values are shown.

The uncropped gel images are provided in Supplementary Fig. 1.

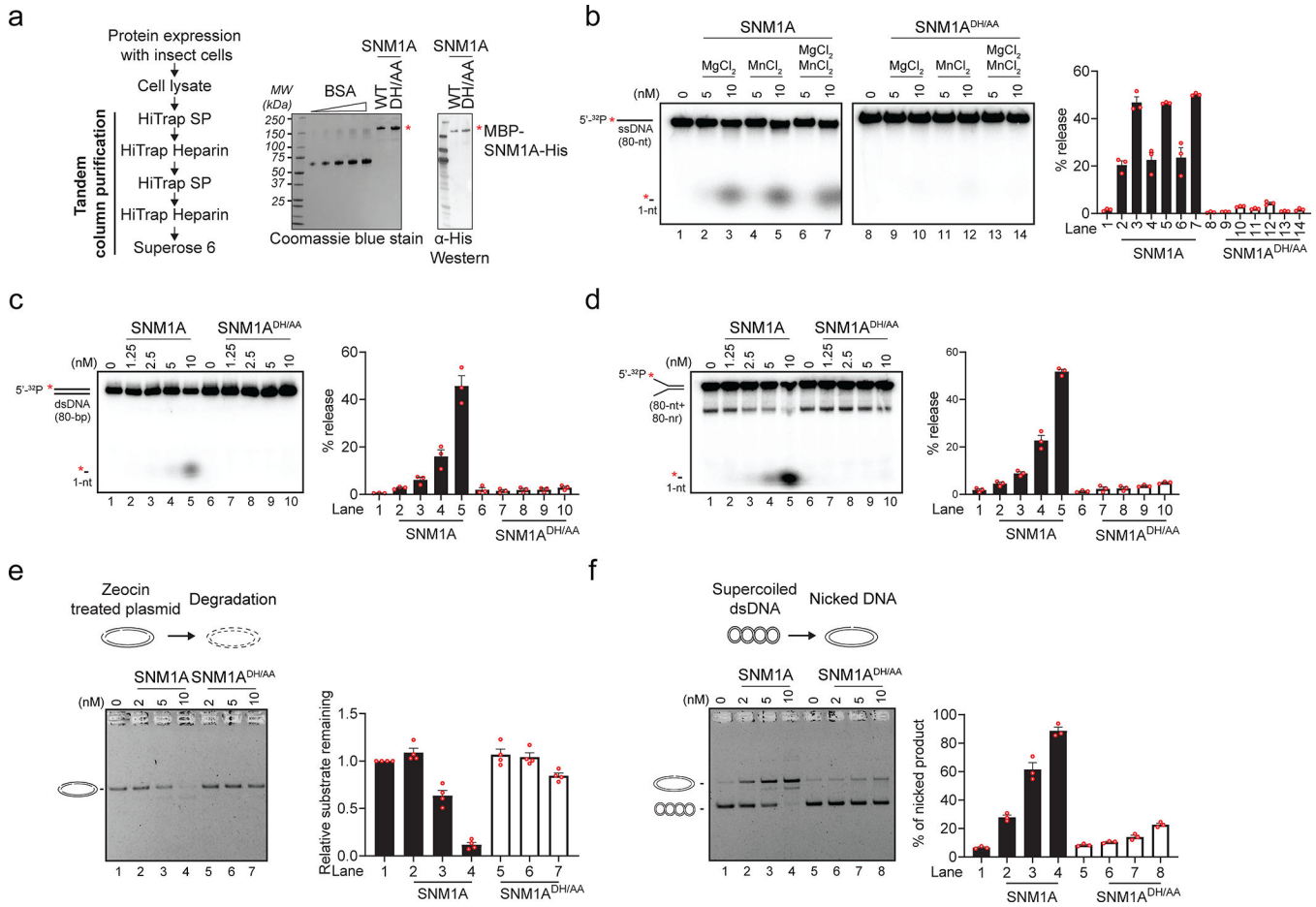

Extended Data Figure 4-related to Figure 3. Endonuclease and exonuclease activities assay with full length SNM1A

a. Left, flow chart summarizing the SNM1A purification scheme. Right, purified SNM1A and SNM1A$^{DH/AA}$, 300 ng each, were analyzed by Coomassie blue staining and Western-blot.

b. SNM1A and SNM1A$^{DH/AA}$ were tested for exonuclease activity using 5' ^{32}P-labeled 80-nt ssDNA as substrate and $MgCl_2$ and/or $MnCl_2$ as indicated. Data (mean ± SEM) from three independent experiments were quantified and shown in the histogram.

c-d. SNM1A and SNM1A$^{DH/AA}$ were tested for exonuclease activity using 5' ^{32}P-labeled 80-bp dsDNA (c) or fork DNA (d) with $MgCl_2$. Data (mean ± SEM) from three independent experiments were quantified and shown in the histogram.

e. SNM1A and SNM1A$^{DH/AA}$ were tested with zeocin treated ϕX174 replicative form DNA and $MgCl_2$. Data (mean ± SEM) from four independent experiments were quantified and shown in the histogram.

f. SNM1A and SNM1A$^{DH/AA}$ were tested with ϕX174 replicative form I (supercoiled) DNA and $MgCl_2$. Data (mean ± SEM) from three independent experiments were quantified and shown in the histogram.

The uncropped gel images are provided in Supplementary Fig. 1.

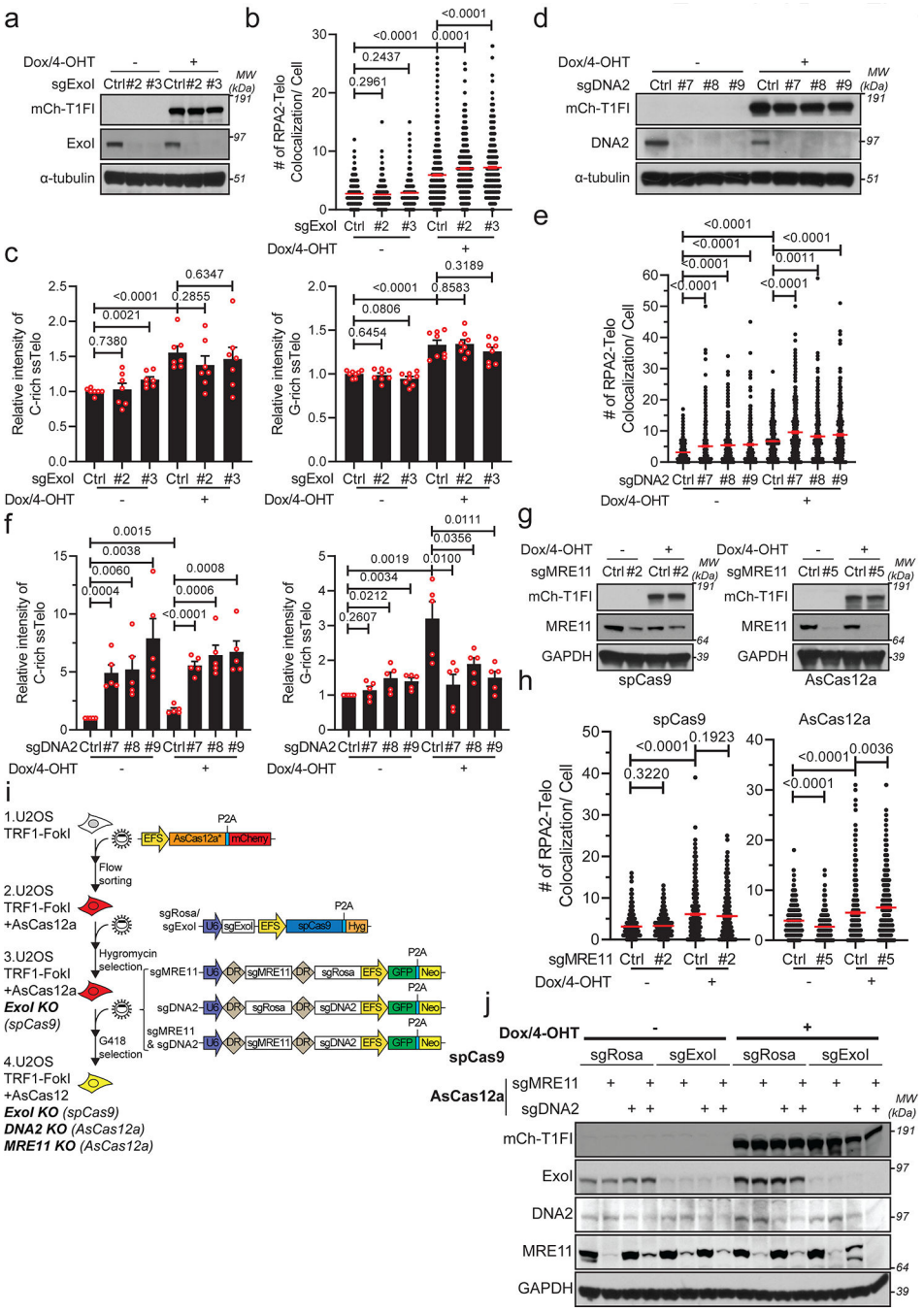

Extended Data Figure 5-related to Figure 3. Canonical double-strand break exonucleases are dispensable for end resection during break induced telomere synthesis

a. Western blot showing human ExoI depletion from U2OS cells with sgRNA targeting Rosa (sgCtrl) or ExoI (sgExoI #2, #3).

b. Quantification of RPA2 and telomere foci colocalization events in U2OS cells with sgRNA targeting Rosa (sgCtrl) or ExoI following TRF1-FokI induction for 2 hrs. Data represent the mean ± SEM of three independent experiments (n = 587, 586, 546, 553,

523, 478 (left to right)). Statistical analyses were performed using an unpaired two-tailed student's *t*-test. *p* values are shown.

c. Quantification of the relative C-rich (Left) and G-rich (Right) single-stranded telomere intensity in U2OS cells with sgRNA targeting ExoI. Data represent the mean ± SEM of two or three independent experiments (n = 7 (left) and n = 8 (right) biological replicates in total). Statistical analyses were performed using an unpaired two-tailed student's *t*-test. *p* values are shown.

d. Western blot showing DNA2 depletion from U2OS cells induced with TRF1-FokI for 2 hrs.

e. Quantification of RPA2 and telomere foci colocalization events in U2OS cells, with gRNAs targeting Rosa (sgCtrl) or DNA2 induced with TRF1-FokI for 2 hrs. Data represent the mean ± SEM of three independent experiments (n = 519, 382, 331, 332, 441, 355, 340, 339 (left to right)). Statistical analyses were performed using an unpaired two-tailed student's *t*-test. *p* values are shown.

f. Quantification of the relative C-rich (Left) and G-rich (Right) single-stranded telomere intensity in U2OS cells that express sgRNA targeting Rosa or DNA2, respectively. Data represent the mean ± SEM of five independent experiments. Statistical analyses were performed using an unpaired two-tailed student's *t*-test. *p* values are shown.

g. Western blot showing MRE11 depletion from U2OS cells using either spCas9 (left panels) or AsCas12a (right panels). TRF1-FokI was induced for 2 hrs.

h. Quantification of RPA2 and telomere foci colocalization events in U2OS cells induced with TRF1-FokI for 2 hrs. Data represent the mean ± SEM of three independent experiments (n = 556, 459, 510, 544 (left) and n = 495, 691, 479, 588 (right) (left to right)). Statistical analyses were performed using an unpaired two-tailed student's *t*-test. *p* values are shown.

i. Schematic of the dual CRISPR/Cas (spCas9 and AsCas12a) mediated deletions of ExoI, DNA2 and MRE11. spCas9 was used for single knockouts and spCas9 + AsCas12a were used for triple knockouts.

j. Western blot showing MRE11, ExoI and DNA2 knock outs individually or in combination with dual CRISPR/Cas system (spCas9 and AsCas12a) from U2OS cells induced with TRF1-FokI for 2 hrs.

The uncropped gel images are provided in Supplementary Fig. 1.

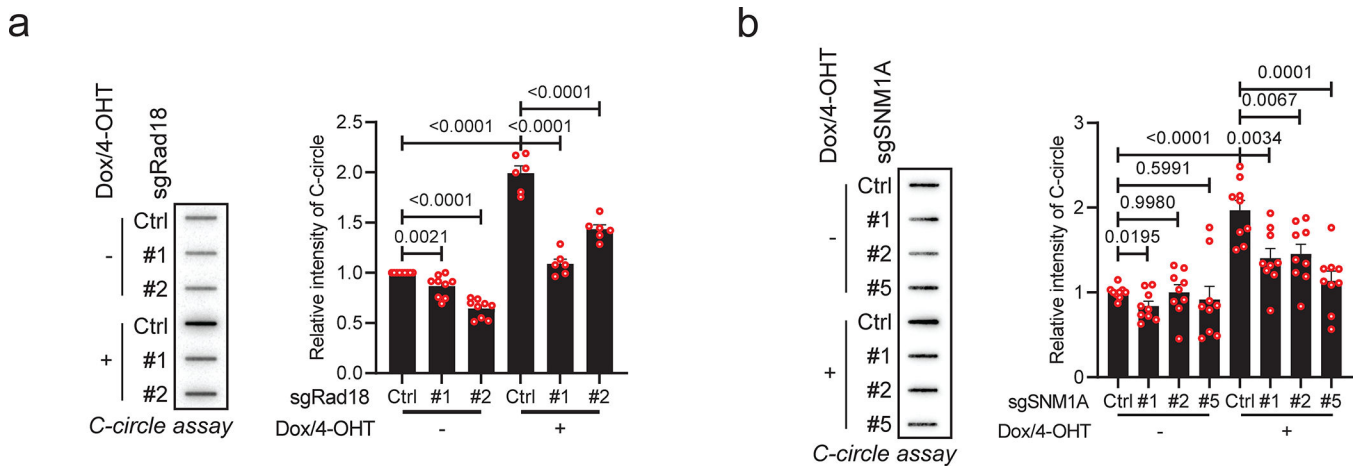

Extended Data Figure 6-related to Figure 4. RAD18 and SNM1A are dispensable for canonical DSBR at telomeres

a. Representative C-circle slot blot and quantification of the relative intensity of C-circles from U2OS cells that express sgRNA targeting Rosa (sgCtrl) or RAD18 (sgRAD18 #1, #2). TRF1-Fok1 was induced for 2 hrs. Data represent the mean ± SEM of three independent experiments (three biological replicates for each independent experiments, n = 9, 9, 9, 6, 6, 6). Statistical analyses were performed using an unpaired two-tailed student's *t*-test. *p* values are shown.

b. Representative C-circle slot blot and quantification of the relative intensity of C-circles from U2OS cells that express sgRNA targeting Rosa (sgCtrl) or SNM1A (sgSNM1A #1, #2, #5). TRF1-Fok1 was induced for 2 hrs. Data represent the mean ± SEM of three independent experiments (three biological replicates for each independent experiments, n = 9, 9, 9, 9, 9, 9). Statistical analyses were performed using an unpaired two-tailed student's *t*-test. *p* values are shown.

The uncropped gel images are provided in Supplementary Fig. 1.

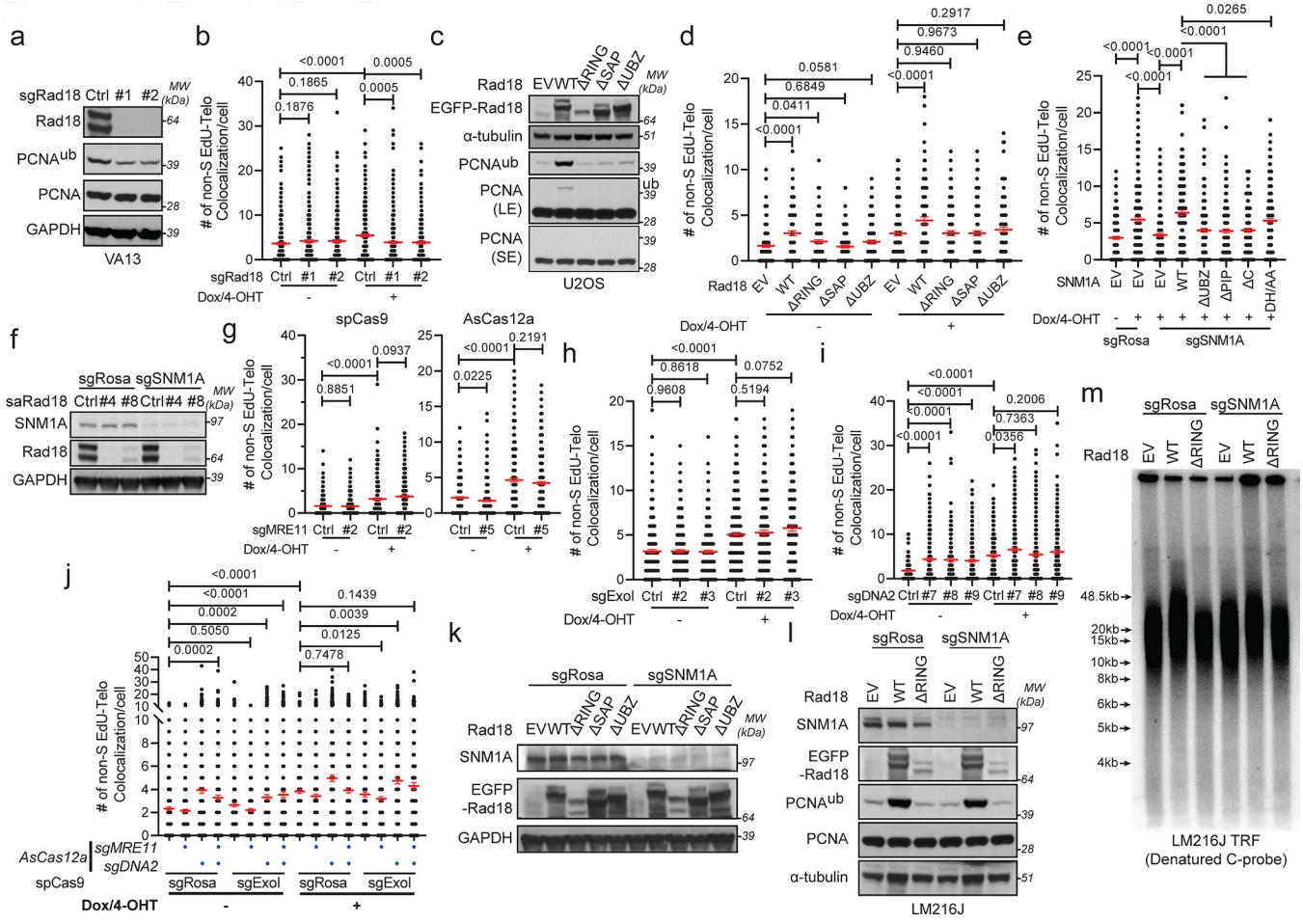

Extended Data Figure 7-related to Figure 5. RAD18 and SNM1A are required for BITS

a. Western blot of PCNA ubiquitination in RAD18 knocked out VA13 cells. VA13 cells were targeted by the indicated sgRNAs and TRF1-FokI was induced with doxycycline + 4-hydroxytamoxifen.

b. Quantification of EdU colocalizing with telomeres in RAD18 knocked out (sgRAD18, #1 and #2 guide RNA) or sgCtrl in VA13 cells following TRF1-FokI for 2.5 hrs in G2 phase. Data represent the mean ± SEM of three independent experiments (n = 340, 341, 291, 323, 365, 277(left to right)). Statistical analyses were performed using an unpaired two-tailed student's *t*-test. *p* values are shown.

c. Western blot of PCNA ubiquitination (Ubiquitylated PCNA (Lys164)) in U2OS cells stably overexpressing RAD18 (or mutants).

d. Quantification of EdU colocalizing with telomeres in U2OS cells stably overexpressing RAD18 (or mutants) following induction with TRF1-FokI for 2.5 hrs in G2 phase. Data represent the mean ± SEM of three independent experiments (n = 164, 123, 149, 134, 143, 148, 125, 125, 136, 134 (left to right)). Statistical analyses were performed using an unpaired two-tailed student's *t*-test. *p* values are shown.

e. Quantification of EdU colocalizing with telomeres in SNM1A knocked out U2OS cells reconstituted with sgRNA resistant SNM1A or mutants. TRF1-FokI was induced for 2.5 hrs in G2 phase. Data represent the mean ± SEM of three independent experiments (n = 202, 237, 222, 167, 233, 207, 166, 239 (left to right)). Statistical analyses were performed using an unpaired two-tailed student's *t*-test. *p* values are shown.

f. Western blot showing endogenous SNM1A and RAD18 depletion in U2OS cells by the dual CRISPR/Cas9 system. SNM1A is targeted by spCas9 with gRNA #2, and RAD18 is targeted by saCas9 with gRNA #4 and #8, respectively. Whole cell extracts were separated with SDS-PAGE and blotted with SNM1A, RAD18 and GAPDH (loading control) antibodies.

g-j. Quantification of EdU colocalizing with telomeres in MRE11, ExoI, and DNA2 that have been knocked out individually or in combination in U2OS cells. TRF1-FokI was induced for 2.5 hrs in G2 phase. Data represent the mean ± SEM of three independent experiments (n = 302, 318, 260, 336 (left) and n = 315, 348, 328, 398 (right) in (g); n = 248, 252, 260, 263, 281, 203 in (h); n = 206, 201, 181, 185, 170, 253, 223, 219 in (i); n = 388, 390, 333, 368, 381, 351, 348, 336, 423, 390, 383, 347, 357, 412, 349, 285 in (j) (left to right)). Statistical analyses were performed using an unpaired two-tailed student's *t*-test. *p* values are shown.

k. Western blot showing wild type RAD18 and mutants overexpression in SNM1A proficient and depleted U2OS cells.

l. Western blot showing wild type Rad18 and mutant overexpression in SNM1A proficient and depleted LM216J cells.

m. Telomere Restriction Fragments (TRF) analysis of telomere length in LM216J cells that overexpress wild type RAD18 or RAD18 mutants in context of SNM1A proficient (sgRosa) or knocked out (sgSNM1A) conditions.

The uncropped gel images are provided in Supplementary Fig. 1.

Extended Data Table 1-

PICh results for DDR pathways in HeLa S3 and U2OS

		HeLa S3				U2OS			
		Exp #1		Exp #2		Exp #1		Exp #2	
	Gene	D450A	WT	D450A	WT	D450A	WT	D450A	WT
Shelterin	TERF2	193	304	140	175	317	245	259	183
	TERF1	433	306	217	185	368	224	264	205
	TINF2	95	116	90	115	125	107	151	108
	TERF2IP	116	203	125	177	235	222	228	158
	POT1	95	109	74	95	84	58	49	45
	TPP1	24	33	21	43	28	23	28	23
MRN Complex	ATM	1	7	0	13	9	9	2	7
	MDC1	0	0	0	0	18	18	8	6
	MRE11	56	140	38	99	68	118	39	121
	RAD50	96	246	46	179	138	208	85	239
	NBN	32	86	30	71	48	84	33	88
Homologous Recombination	BRCA1	0	6	0	3	10	18	1	3
	BARD1	0	1	0	0	1	5	1	8
	MMS22L	1	20	1	9	1	16	3	34
	TONSL	12	30	6	13	10	27	8	54
	RAD51	0	3	0	4	0	2	1	4
Non-homologous End-Joining	PRKDC	191	286	108	183	192	172	123	126
	XRCC6	120	130	64	95	128	117	111	133
	XRCC5	67	98	51	77	115	97	88	110
	TP53BP1	0	0	3	11	9	15	1	5
	RIF1	0	10	0	9	19	19	7	0
	XRCC4	0	0	1	2	0	2	1	5
	Lig4	0	0	0	0	0	0	0	0
	DCLRE1C	0	0	0	0	0	0	0	0
	SFPQ	20	28	10	12	40	32	22	25
	NONO	19	17	21	21	26	35	30	24
	XLF/NHEJ1	0	0	0	0	0	0	0	0
	SMCHD1	59	39	30	22	66	43	65	41
Break induced telomere synthesis	RFC1	5	36	4	25	22	46	15	86
	RFC2	5	23	7	19	12	20	9	31
	RFC3	5	13	2	14	5	14	1	10
	RFC4	14	21	8	17	11	18	5	37
	RFC5	5	19	8	15	9	13	5	22
	PCNA	26	141	23	157	27	94	25	130
	POLD1	30	62	17	39	13	17	19	33
	POLD2	10	21	10	16	8	9	5	8
	POLD3	4	12	3	9	3	4	3	5

		HeLa S3				U2OS			
		Exp #1		Exp #2		Exp #1		Exp #2	
	Gene	D450A	WT	D450A	WT	D450A	WT	D450A	WT
Conventional Replisome	CDC45	0	0	0	0	2	2	0	2
	MCM2	62	70	48	61	102	85	89	63
	MCM3	57	73	33	52	124	95	101	58
	MCM4	33	64	38	57	83	57	87	61
	MCM5	31	52	29	43	69	58	74	46
	MCM6	46	76	28	34	77	67	43	31
	MCM7	75	77	48	55	126	99	92	66
	GINS1	2	3	2	3	5	4	1	2
	GINS2	0	4	2	2	4	3	0	2
	GINS3	1	3	0	2	5	5	0	1
	GINS4	3	5	3	5	9	4	6	2
	POLA1	0	2	3	14	17	8	9	9
	POLA2	0	5	0	0	3	1	0	0
	POLE	0	1	1	3	17	15	11	10
	POLE3	1	1	3	3	3	4	0	0
	POLE4	0	0	0	2	1	0	0	0
Alternative End Joining	POLB	2	6	2	8	2	8	0	9
	POLH	0	0	0	0	1	0	0	0
	PARP1	81	95	41	53	77	70	63	52
	PARP2	1	2	0	0	0	0	0	1
	LIG1	0	54	1	26	0	20	8	31
	LIG3	13	54	10	41	8	62	9	76
	XRCC1	7	20	11	17	8	31	5	30
	ERCC1	8	8	8	11	21	19	18	16
	ERCC4	36	46	31	42	66	88	60	49
	FEN1	27	41	19	42	35	33	25	43
ATR signaling pathway	APEX1	4	11	11	11	26	22	5	9
	ATR	0	66	0	37	28	56	20	38
	ATRIP	0	7	0	5	2	16	1	6
	TOPBP1	0	39	2	25	24	44	14	36
	RBBP8	0	1	0	4	0	5	2	8
	RPA1	96	149	77	128	107	98	119	114
	RPA2	21	26	26	37	25	28	29	22
	RPA3	9	8	5	9	5	4	6	4
	RAD9A	10	10	3	9	3	8	5	10
	RAD1	6	11	4	15	6	6	3	2
	HUS1	1	3	2	3	4	4	3	2
Fanconi Anemia	FANCD2	1	56	0	17	45	53	23	32
	FANCI	6	66	2	26	61	72	25	39
Exonuclease	EXO1	0	0	0	0	0	0	0	0

		HeLa S3				U2OS			
		Exp #1		Exp #2		Exp #1		Exp #2	
	Gene	D450A	WT	D450A	WT	D450A	WT	D450A	WT
DNA damage tolerance	DCLRE1A	0	56	0	35	4	35	1	31
	DCLRE1B	33	49	8	21	69	50	47	25
	Rad18	2	14	1	10	12	20	2	21
	HLTF	7	23	10	19	0	1	0	0
	SHPRH	0	0	0	0	0	0	0	0
	ZRANB3	0	0	0	0	0	0	0	0
Mismatch repair	MSH2	50	116	40	91	39	91	43	162
	MSH3	2	24	0	16	2	6	0	5
	MSH6	47	146	31	81	66	120	56	159
	MLH1	2	1	0	2	6	2	5	3

Supplementary Material

Refer to Web version on PubMed Central for supplementary material.

Acknowledgments

We thank J. Déjardin (CNRS, France) for guidance on performing PICh experiments. We thank members of the Greenberg lab for critical discussion. This work was supported by NIH RO1 GM1101149 and RO1 CA174904, and Bloom Syndrome Grant Program BLOOM-22–004-01 to R.A.G., RO1 ES007061 and R35 CA241801 to P.S., and a Gray Foundation Team Science Award to R.A.G. and P.S.; R50CA265315 to Y.K; and an AFCRI funded postdoctoral fellowship to T.Z.

Data availability

All data are available in the main paper, supplementary information. Source data and uncropped gel images are provided with this paper. All reagents are available from the corresponding author upon reasonable request.

References

1. Dilley RL et al. Break-induced telomere synthesis underlies alternative telomere maintenance. Nature 539, 54–58, doi:10.1038/nature20099 (2016). [PubMed: 27760120]
2. Roumelioti FM et al. Alternative lengthening of human telomeres is a conservative DNA replication process with features of break-induced replication. EMBO Rep 17, 1731–1737, doi:10.15252/embr.201643169 (2016). [PubMed: 27760777]
3. Kramara J, Osia B & Malkova A Break-Induced Replication: The Where, The Why, and The How. Trends Genet 34, 518–531, doi:10.1016/j.tig.2018.04.002 (2018). [PubMed: 29735283]
4. Epum EA & Haber JE DNA replication: the recombination connection. Trends Cell Biol 32, 45–57, doi:10.1016/j.tcb.2021.07.005 (2022). [PubMed: 34384659]
5. Wu X & Malkova A Break-induced replication mechanisms in yeast and mammals. Curr Opin Genet Dev 71, 163–170, doi:10.1016/j.gde.2021.08.002 (2021). [PubMed: 34481360]
6. Dejardin J & Kingston RE Purification of proteins associated with specific genomic Loci. Cell 136, 175–186, doi:10.1016/j.cell.2008.11.045 (2009). [PubMed: 19135898]
7. Al-Zain AM & Symington LS The dark side of homology-directed repair. DNA Repair (Amst) 106, 103181, doi:10.1016/j.dnarep.2021.103181 (2021). [PubMed: 34311272]

8. Costantino L et al. Break-induced replication repair of damaged forks induces genomic duplications in human cells. Science 343, 88–91, doi:10.1126/science.1243211 (2014). [PubMed: 24310611]
9. Smith CE, Llorente B & Symington LS Template switching during break-induced replication. Nature 447, 102–105, doi:10.1038/nature05723 (2007). [PubMed: 17410126]
10. Cho NW, Dilley RL, Lampson MA & Greenberg RA Interchromosomal homology searches drive directional ALT telomere movement and synapsis. Cell 159, 108–121, doi:10.1016/j.cell.2014.08.030 (2014). [PubMed: 25259924]
11. de Lange T Shelterin: the protein complex that shapes and safeguards human telomeres. Genes Dev 19, 2100–2110, doi:10.1101/gad.1346005 (2005). [PubMed: 16166375]
12. Attali I, Botchan MR & Berger JM Structural Mechanisms for Replicating DNA in Eukaryotes. Annu Rev Biochem 90, 77–106, doi:10.1146/annurev-biochem-090120-125407 (2021). [PubMed: 33784179]
13. Lydeard JR, Jain S, Yamaguchi M & Haber JE Break-induced replication and telomerase-independent telomere maintenance require Pol32. Nature 448, 820–823, doi:10.1038/nature06047 (2007). [PubMed: 17671506]
14. Doksani Y & de Lange T Telomere-Internal Double-Strand Breaks Are Repaired by Homologous Recombination and PARP1/Lig3-Dependent End-Joining. Cell Rep 17, 1646–1656, doi:10.1016/j.celrep.2016.10.008 (2016). [PubMed: 27806302]
15. Mao P et al. Homologous recombination-dependent repair of telomeric DSBs in proliferating human cells. Nat Commun 7, 12154, doi:10.1038/ncomms12154 (2016). [PubMed: 27396625]
16. Cesare AJ et al. Spontaneous occurrence of telomeric DNA damage response in the absence of chromosome fusions. Nat Struct Mol Biol 16, 1244–1251, doi:10.1038/nsmb.1725 (2009). [PubMed: 19935685]
17. Flynn RL et al. Alternative lengthening of telomeres renders cancer cells hypersensitive to ATR inhibitors. Science 347, 273–277, doi:10.1126/science.1257216 (2015). [PubMed: 25593184]
18. Baddock HT et al. The SNM1A DNA repair nuclease. DNA Repair (Amst) 95, 102941, doi:10.1016/j.dnarep.2020.102941 (2020). [PubMed: 32866775]
19. Buzon B, Grainger R, Huang S, Rzadki C & Junop MS Structure-specific endonuclease activity of SNM1A enables processing of a DNA interstrand crosslink. Nucleic Acids Res 46, 9057–9066, doi:10.1093/nar/gky759 (2018). [PubMed: 30165656]
20. Zou L & Elledge SJ Sensing DNA damage through ATRIP recognition of RPA-ssDNA complexes. Science 300, 1542–1548, doi:10.1126/science.1083430 (2003). [PubMed: 12791985]
21. Cimprich KA & Cortez D ATR: an essential regulator of genome integrity. Nat Rev Mol Cell Biol 9, 616–627, doi:10.1038/nrm2450 (2008). [PubMed: 18594563]
22. Verma P et al. RAD52 and SLX4 act nonepistatically to ensure telomere stability during alternative telomere lengthening. Genes Dev 33, 221–235, doi:10.1101/gad.319723.118 (2019). [PubMed: 30692206]
23. Yang Z, Takai KK, Lovejoy CA & de Lange T Break-induced replication promotes fragile telomere formation. Genes Dev 34, 1392–1405, doi:10.1101/gad.328575.119 (2020). [PubMed: 32883681]
24. Zhang JM, Genois MM, Ouyang J, Lan L & Zou L Alternative lengthening of telomeres is a self-perpetuating process in ALT-associated PML bodies. Mol Cell 81, 1027–1042 e1024, doi:10.1016/j.molcel.2020.12.030 (2021). [PubMed: 33453166]
25. Niimi A et al. Regulation of proliferating cell nuclear antigen ubiquitination in mammalian cells. Proc Natl Acad Sci U S A 105, 16125–16130, doi:10.1073/pnas.0802727105 (2008). [PubMed: 18845679]
26. Kannouche PL, Wing J & Lehmann AR Interaction of human DNA polymerase eta with monoubiquitinated PCNA: a possible mechanism for the polymerase switch in response to DNA damage. Mol Cell 14, 491–500, doi:10.1016/s1097-2765(04)00259-x (2004). [PubMed: 15149598]
27. Huang J et al. RAD18 transmits DNA damage signalling to elicit homologous recombination repair. Nat Cell Biol 11, 592–603, doi:10.1038/ncb1865 (2009). [PubMed: 19396164]
28. Chang DJ & Cimprich KA DNA damage tolerance: when it's OK to make mistakes. Nat Chem Biol 5, 82–90, doi:10.1038/nchembio.139 (2009). [PubMed: 19148176]

29. Nambiar TS et al. Stimulation of CRISPR-mediated homology-directed repair by an engineered RAD18 variant. Nat Commun 10, 3395, doi:10.1038/s41467-019-11105-z (2019). [PubMed: 31363085]
30. Lydeard JR et al. Break-induced replication requires all essential DNA replication factors except those specific for pre-RC assembly. Genes Dev 24, 1133–1144, doi:10.1101/gad.1922610 (2010). [PubMed: 20516198]
31. Yang K, Moldovan GL & D'Andrea AD RAD18-dependent recruitment of SNM1A to DNA repair complexes by a ubiquitin-binding zinc finger. J Biol Chem 285, 19085–19091, doi:10.1074/jbc.M109.100032 (2010). [PubMed: 20385554]
32. Syvaoja J et al. DNA polymerases alpha, delta, and epsilon: three distinct enzymes from HeLa cells. Proc Natl Acad Sci U S A 87, 6664–6668, doi:10.1073/pnas.87.17.6664 (1990). [PubMed: 1975694]
33. Oganesian L & Karlseder J Mammalian 5' C-rich telomeric overhangs are a mark of recombination-dependent telomere maintenance. Mol Cell 42, 224–236, doi:10.1016/j.molcel.2011.03.015 (2011). [PubMed: 21504833]
34. Nabetani A & Ishikawa F Unusual telomeric DNAs in human telomerase-negative immortalized cells. Mol Cell Biol 29, 703–713, doi:10.1128/MCB.00603-08 (2009). [PubMed: 19015236]
35. Zhang T et al. Strand break-induced replication fork collapse leads to C-circles, C-overhangs and telomeric recombination. PLoS Genet 15, e1007925, doi:10.1371/journal.pgen.1007925 (2019). [PubMed: 30716077]
36. Sengerova B et al. Characterization of the human SNM1A and SNM1B/Apollo DNA repair exonucleases. J Biol Chem 287, 26254–26267, doi:10.1074/jbc.M112.367243 (2012). [PubMed: 22692201]
37. Wang AT et al. Human SNM1A and XPF-ERCC1 collaborate to initiate DNA interstrand cross-link repair. Genes Dev 25, 1859–1870, doi:10.1101/gad.15699211 (2011). [PubMed: 21896658]
38. Zhu Z, Chung WH, Shim EY, Lee SE & Ira G Sgs1 helicase and two nucleases Dna2 and Exo1 resect DNA double-strand break ends. Cell 134, 981–994, doi:10.1016/j.cell.2008.08.037 (2008). [PubMed: 18805091]
39. Rossi SE, Foiani M & Giannattasio M Dna2 processes behind the fork long ssDNA flaps generated by Pif1 and replication-dependent strand displacement. Nat Commun 9, 4830, doi:10.1038/s41467-018-07378-5 (2018). [PubMed: 30446656]
40. Sfeir A et al. Mammalian telomeres resemble fragile sites and require TRF1 for efficient replication. Cell 138, 90–103, doi:10.1016/j.cell.2009.06.021 (2009). [PubMed: 19596237]
41. Gilson E & Geli V How telomeres are replicated. Nat Rev Mol Cell Biol 8, 825–838, doi:10.1038/nrm2259 (2007). [PubMed: 17885666]
42. Garcia-Exposito L et al. Proteomic Profiling Reveals a Specific Role for Translesion DNA Polymerase eta in the Alternative Lengthening of Telomeres. Cell Rep 17, 1858–1871, doi:10.1016/j.celrep.2016.10.048 (2016). [PubMed: 27829156]
43. Zhang H & Lawrence CW The error-free component of the RAD6/RAD18 DNA damage tolerance pathway of budding yeast employs sister-strand recombination. Proc Natl Acad Sci U S A 102, 15954–15959, doi:10.1073/pnas.0504586102 (2005). [PubMed: 16247017]
44. Branzei D, Vanoli F & Foiani M SUMOylation regulates Rad18-mediated template switch. Nature 456, 915–920, doi:10.1038/nature07587 (2008). [PubMed: 19092928]
45. Vanoli F, Fumasoni M, Szakal B, Maloisel L & Branzei D Replication and recombination factors contributing to recombination-dependent bypass of DNA lesions by template switch. PLoS Genet 6, e1001205, doi:10.1371/journal.pgen.1001205 (2010). [PubMed: 21085632]
46. Stafa A, Donnianni RA, Timashev LA, Lam AF & Symington LS Template switching during break-induced replication is promoted by the Mph1 helicase in Saccharomyces cerevisiae. Genetics 196, 1017–1028, doi:10.1534/genetics.114.162297 (2014). [PubMed: 24496010]
47. Anand RP et al. Chromosome rearrangements via template switching between diverged repeated sequences. Genes Dev 28, 2394–2406, doi:10.1101/gad.250258.114 (2014). [PubMed: 25367035]
48. Fallet E et al. Length-dependent processing of telomeres in the absence of telomerase. Nucleic Acids Res 42, 3648–3665, doi:10.1093/nar/gkt1328 (2014). [PubMed: 24393774]

49. Lowden MR, Flibotte S, Moerman DG & Ahmed S DNA synthesis generates terminal duplications that seal end-to-end chromosome fusions. Science 332, 468–471, doi:10.1126/science.1199022 (2011). [PubMed: 21512032]
50. Stivison EA, Young KJ & Symington LS Interstitial telomere sequences disrupt break-induced replication and drive formation of ectopic telomeres. Nucleic Acids Res 48, 12697–12710, doi:10.1093/nar/gkaa1081 (2020). [PubMed: 33264397]
51. Liu L et al. Tracking break-induced replication shows that it stalls at roadblocks. Nature 590, 655–659, doi:10.1038/s41586-020-03172-w (2021). [PubMed: 33473214]
52. Hejna J, Philip S, Ott J, Faulkner C & Moses R The hSNM1 protein is a DNA 5'-exonuclease. Nucleic Acids Res 35, 6115–6123, doi:10.1093/nar/gkm530 (2007). [PubMed: 17804464]
53. Verma P et al. ALC1 links chromatin accessibility to PARP inhibitor response in homologous recombination-deficient cells. Nat Cell Biol 23, 160–171, doi:10.1038/s41556-020-00624-3 (2021). [PubMed: 33462394]
54. Gier RA et al. High-performance CRISPR-Cas12a genome editing for combinatorial genetic screening. Nat Commun 11, 3455, doi:10.1038/s41467-020-17209-1 (2020). [PubMed: 32661245]
55. Kan SL, Saksouk N & Dejardin J Proteome Characterization of a Chromatin Locus Using the Proteomics of Isolated Chromatin Segments Approach. Methods Mol Biol 1550, 19–33, doi:10.1007/978-1-4939-6747-6_3 (2017). [PubMed: 28188520]
56. Zhang T et al. Looping-out mechanism for resolution of replicative stress at telomeres. EMBO reports 18, 1412–1428 (2017). [PubMed: 28615293]
57. Verma P, Dilley RL, Gyparaki MT & Greenberg RA Direct Quantitative Monitoring of Homology-Directed DNA Repair of Damaged Telomeres. Methods Enzymol 600, 107–134, doi:10.1016/bs.mie.2017.11.010 (2018). [PubMed: 29458755]
58. Lippert TP et al. Oncogenic herpesvirus KSHV triggers hallmarks of alternative lengthening of telomeres. Nat Commun 12, 512, doi:10.1038/s41467-020-20819-4 (2021). [PubMed: 33479235]
59. Zhao Y, Shay JW & Wright WE Telomere G-overhang length measurement method 1: the DSN method. *Methods* Mol Biol 735, 47–54, doi:10.1007/978-1-61779-092-8_5 (2011).
60. Henson JD et al. DNA C-circles are specific and quantifiable markers of alternative-lengthening-of-telomeres activity. Nat Biotechnol 27, 1181–1185, doi:10.1038/nbt.1587 (2009). [PubMed: 19935656]
61. Pastwa E, Neumann RD & Winters TA In vitro repair of complex unligatable oxidatively induced DNA double-strand breaks by human cell extracts. Nucleic Acids Res 29, E78, doi:10.1093/nar/29.16.e78 (2001). [PubMed: 11504886]

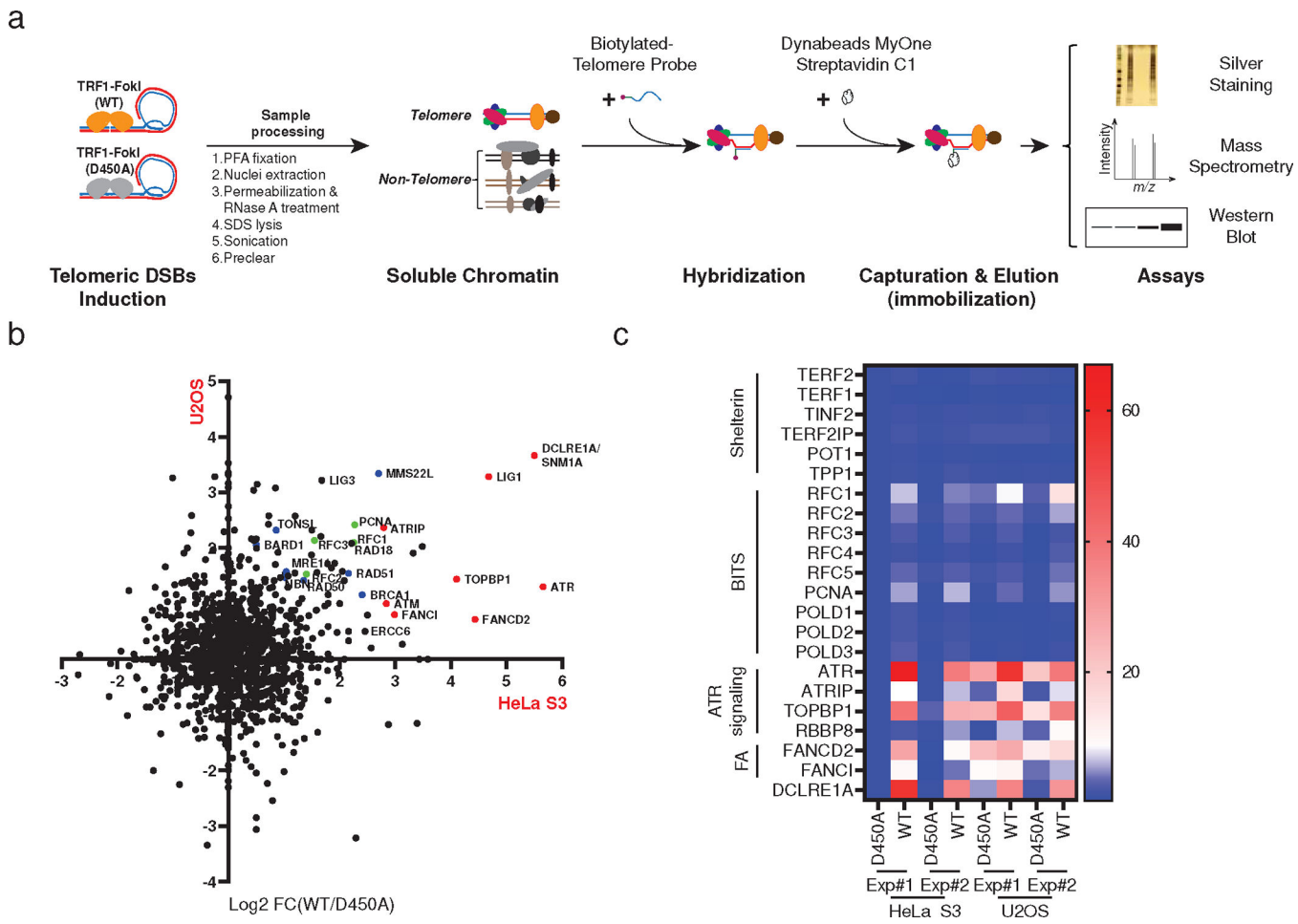

Figure 1. Telomere double strand breaks activate homology directed repair, ATR signaling and Fanconi Anemia pathways

a. Schematic of Proteomics of Isolated Chromatin segments (PICh) to define the telomere specific double strand break (DSB) response proteome profile. Inducible TRF1-FokI (WT) creates synchronous telomere specific DSBs, while TRF1-FokI (D450A, nuclease dead) was used as a control. Fractionated and pre-cleared chromatin was hybridized to a biotinylated telomeric probe, and then captured on magnetic beads. Telomere associated proteins were analyzed by silver staining, western blot, and mass spectrometry. **b**. Scatterplot of telomere specific DSB response proteome profile enriched by PICh in U2OS and HeLa S3 cells, respectively. Mass Spectrometry data was shown in Supplementary Table 1. Scatterplot of $\log_2$ (WT+1)/(D450A+1) of total peptide number of mass spectrometry results comparing the telomere associated proteomics from two independent experiments in HeLa S3 (x-axis) and U2OS (y-axis), respectively. **c**. Heatmap showing enrichment of ATR signaling and Fanconi Anemia pathways at damaged telomeres. Peptides numbers are normalized to TRF1-FokI (D450A, Exp#1).

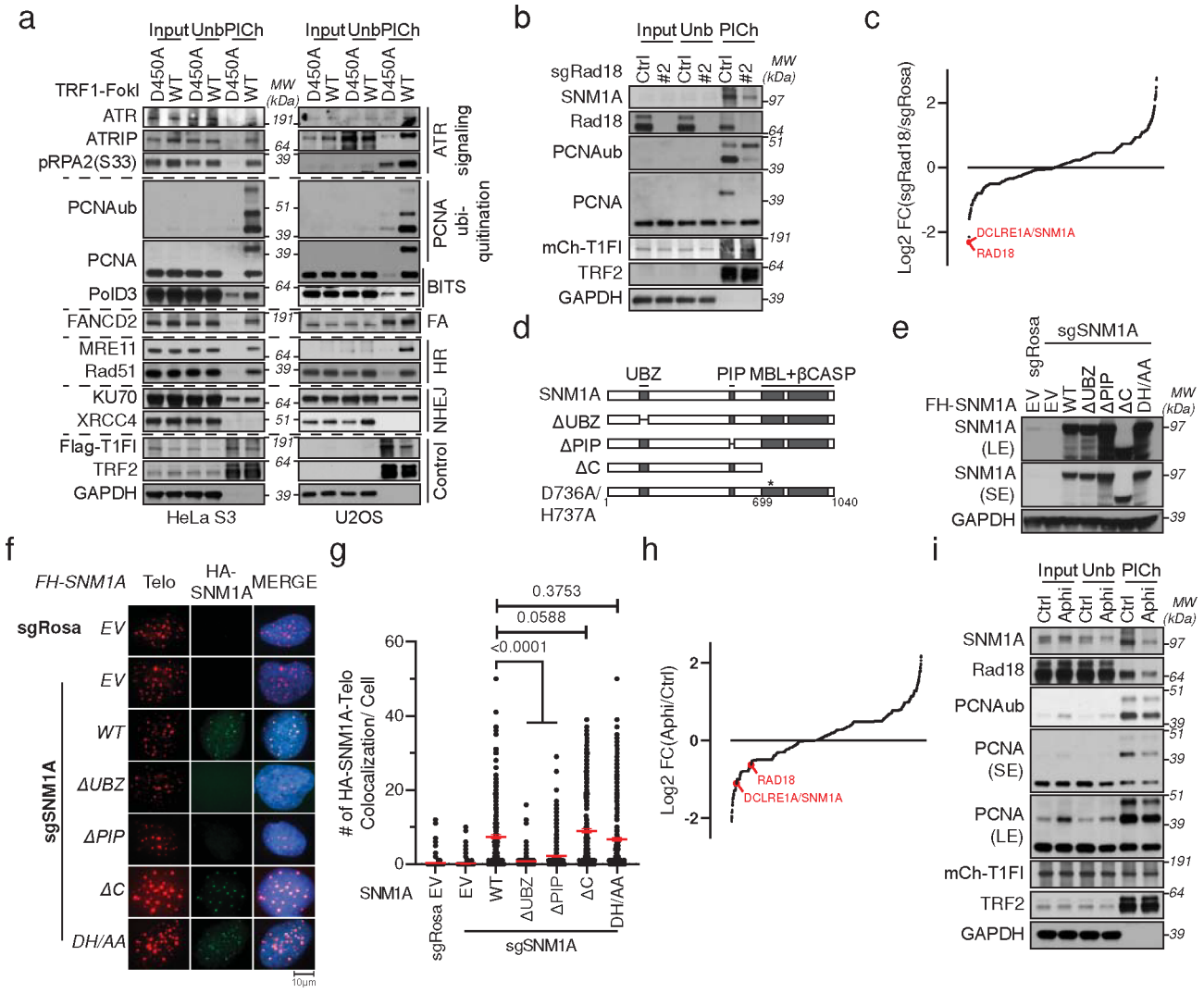

Figure 2. Break induced telomere synthesis promotes RAD18 dependent PCNA-Ub-SNM1A interaction at damaged telomeres.

a. Representative DNA damage response factors by western blot (WB) from PICh experiments in Hela S3 and U2OS. “Input”, “Unb (unbound)” and “PICh” fractions of cells expressing TRF1-FokI (D450A and WT), were separated by SDS-PAGE and blotted with the indicated antibodies in HeLa S3 and U2OS cells. **b.** PICh-WB for telomere associated proteins**. c.** Scatterplot of the telomere specific DSB response proteome profile enriched by PICh in sgRAD18 or sgRosa U2OS cells induced with TRF1-FokI. Mass Spectrometry data was shown in Supplementary Table 2. RAD18 and SNM1A (DCLRE1A) are highlighted. Scatterplot of $\log_2$ (sgRAD18+1)/(sgCtrl+1) of total peptide number from two independent experiments. **d.** Schematic of SNM1A full length and deletion mutant cDNAs used to reconstitute U2OS cells. **e.** Western blot of SNM1A reconstitution in U2OS cells. **f.** Representative IF-FISH images of ectopic SNM1A (or mutants, detected by anti-HA) colocalization with telomere (Telo) in U2OS cells after induction with TRF1-FokI for 2 hrs. **g.** Quantification of (**f**) for number of SNM1A (anti-HA) and telomere foci colocalization events in U2OS cells induced with TRF1-FokI for 2 hrs. Data represent the

mean ± SEM of three independent experiments (n = 262, 313, 248, 232, 274, 294, 353 cells were counted (left to right)). Statistical analyses are done with unpaired two-tailed student's *t*-test. *p* values are shown. **h.** Scatterplot of telomere specific DSB response proteome enriched by PICh in HeLa S3 cells induced with TRF1-FokI for 2 hrs +/− 15 μM aphidicolin (Aphi). Scatterplot of $\log_2$ (Aphi+1)/(Ctrl+1) of total peptide number from two independent experiments. Mass Spectrometry data was shown in Supplementary Table 3. **i.** PICh-WB for telomere associated RAD18, SNM1A, PCNA, ubiquitinated PCNA (PCNAub, Ubiquityl PCNA (Lys164)) in HeLa S3 cells induced with TRF1-FokI for 2 hrs +/− 15 μM aphidicolin (Aphi). The uncropped gel images are provided in Supplementary Fig. 1.

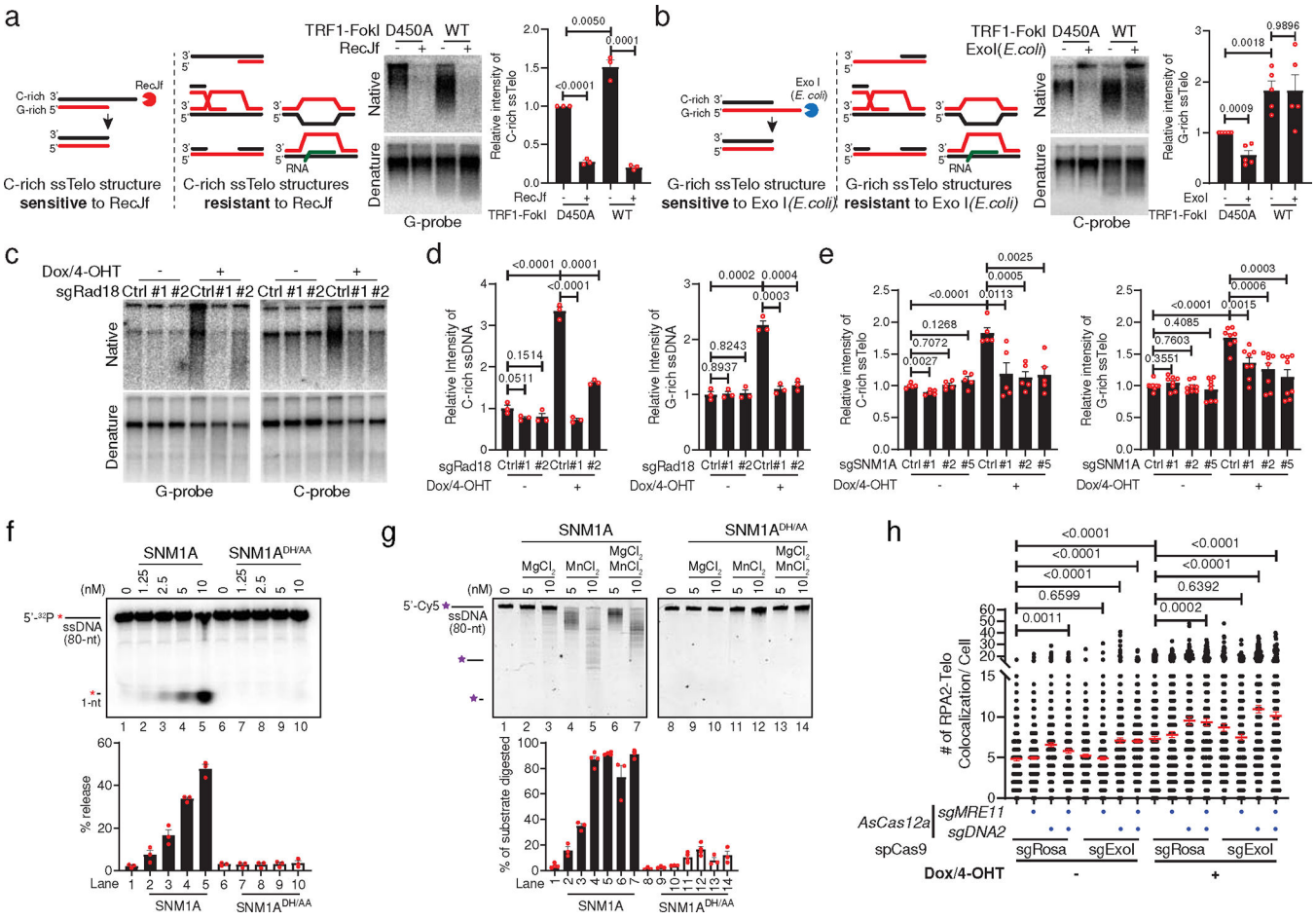

Figure 3. RAD18 and SNM1A are required for end resection during break induced telomere synthesis.

a-b. (left) potential ssDNA telomere structures that are sensitive or resistant to RecJf (**a**) *E. coli* ExoI (**b**) digestion, (right) in-gel hybridization and quantification of telomere content with ^{32}P-labeled telomeric G-probe (**a**) or C-probe (**b**) in U2OS cells following TRF1-FokI (D450A, WT) induction for 2 hrs. **c.** In-gel hybridization of telomere content from U2OS cells under native and denatured conditions with ^{32}P-labeled telomeric G-probe and C-probe, respectively. TRF1-FokI induction by Dox/4-OHT was performed for 2 hrs in U2OS cells expressing sgRNA targeting Rosa (sgCtrl) or RAD18 (sgRAD18 #1, #2). **d-e.** Quantification of relative C-rich (Left) and G-rich (Right) single-stranded telomere intensity, in U2OS cells with sgRNA targeting RAD18 (**d**) and SNM1A (**e**), respectively. Data represents the mean ± SEM of "Relative intensity of native signal to denatured signal" calculated from three or five independent experiments (3 (**a**), 5 (**b**), 3 (**d**), 5 or 8 (**e**) biological replicates included). **f**. SNM1A and SNM1A$^{DH/AA}$ proteins were tested for exonuclease activity using 5' ^{32}P-labeled 80-nt ssDNA with $MgCl_2$. **g**. The endonuclease activity of SNM1A and SNM1A$^{DH/AA}$ proteins were tested with 5' Cy5-labeled 80-nt ssDNA with $MgCl_2$ and/or $MnCl_2$, as indicated. For (**f**) and (**g**), data (mean ± SEM) from three (or four) independent experiments were quantified and presented in the histogram. **h.** Quantification of RPA2 and telomere foci colocalization events in U2OS cells harboring

single or combined knockouts of MRE11, ExoI or DNA2. Data represents the mean ± SEM of three independent experiments (n = 313, 354, 305, 268, 319, 329, 280, 362, 304, 284, 276, 271, 265, 289, 346, 255 cells were counted (left to right)). Statistical analyses were performed using the unpaired two-tailed student's *t*-test. *p* values are shown. The uncropped gel images are provided in Supplementary Fig. 1.

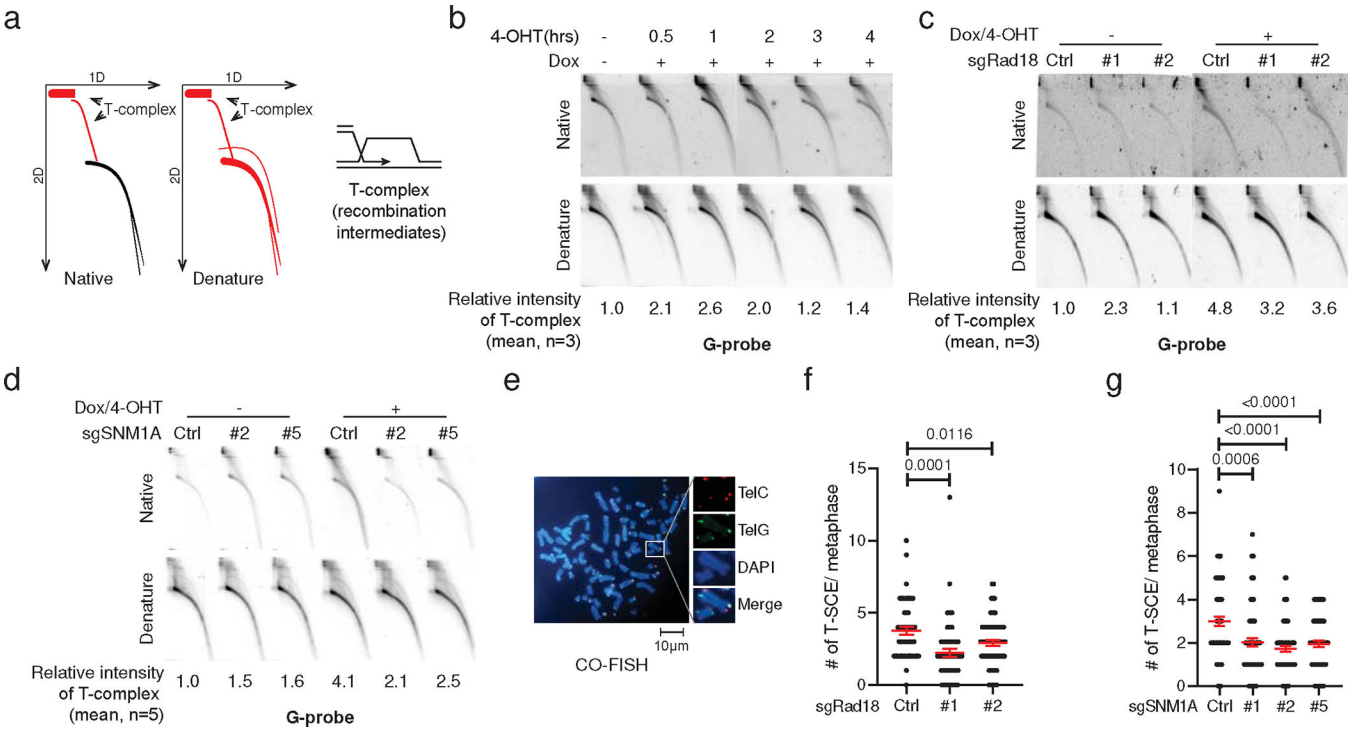

Figure 4. RAD18 and SNM1A are required for the formation of complex recombination intermediates during break induced telomere synthesis.

a. Schematic of the T-complex structure (highlighted), representing the recombination intermediates that are resolved by neutral-neutral 2D gel electrophoresis. **b**. In-gel hybridization of neutral-neutral 2D gel electrophoresis of T-complexes in U2OS treated with TRF1-FokI for the indicated duration. Hybridization was performed with a ^{32}P-labeled telomeric G-probe under native and denaturing conditions. Quantification of "Relative intensity of T-complex" is performed by (T complex signal detected under native hybridization (highlighted in red)/ total abundance of telomere signal detected under denatured condition (highlighted in red)). The mean of "Relative intensity of T-complex" from 3 independent experiments was quantified and noted below samples. **c-d.** In-gel hybridization of neutral-neutral 2D gel separated T-complexes in U2OS cells expressing sgRNAs targeting RAD18 (**c**) or SNM1A (**d**) following treatment with TRF1-FokI for 2 hrs. The average of "Relative intensity of T-complex" of 3 (**c**) or 5 (**d**) independent experiments was quantified and noted below samples. **e.** Representative image of chromosome orientation FISH (CO-FISH) on metaphase spread of U2OS cells. Telomeres were probed with TelG-Alexa488 (Green) and TelC-Cy3 (Red) sequentially, and chromosomes are counterstained with DAPI (Blue). Enlarged images indicate T-SCE events (yellow, colocalization of TelC and TelG probes)**. f-g.** Quantification of T-SCE per metaphase in U2OS cells with sgRNA targeting RAD18 (**f**) or SNM1A (**g**), respectively. Data represents the mean ± SEM of two independent metaphase spread experiments (n = 49, 62, 69 in (**f**) and n = 73, 82, 68, 79 in (**g**) (left to right)). Statistical analyses using an unpaired two-tailed student's *t*-test. *p* values are shown. The uncropped gel images are provided in Supplementary Fig. 1.

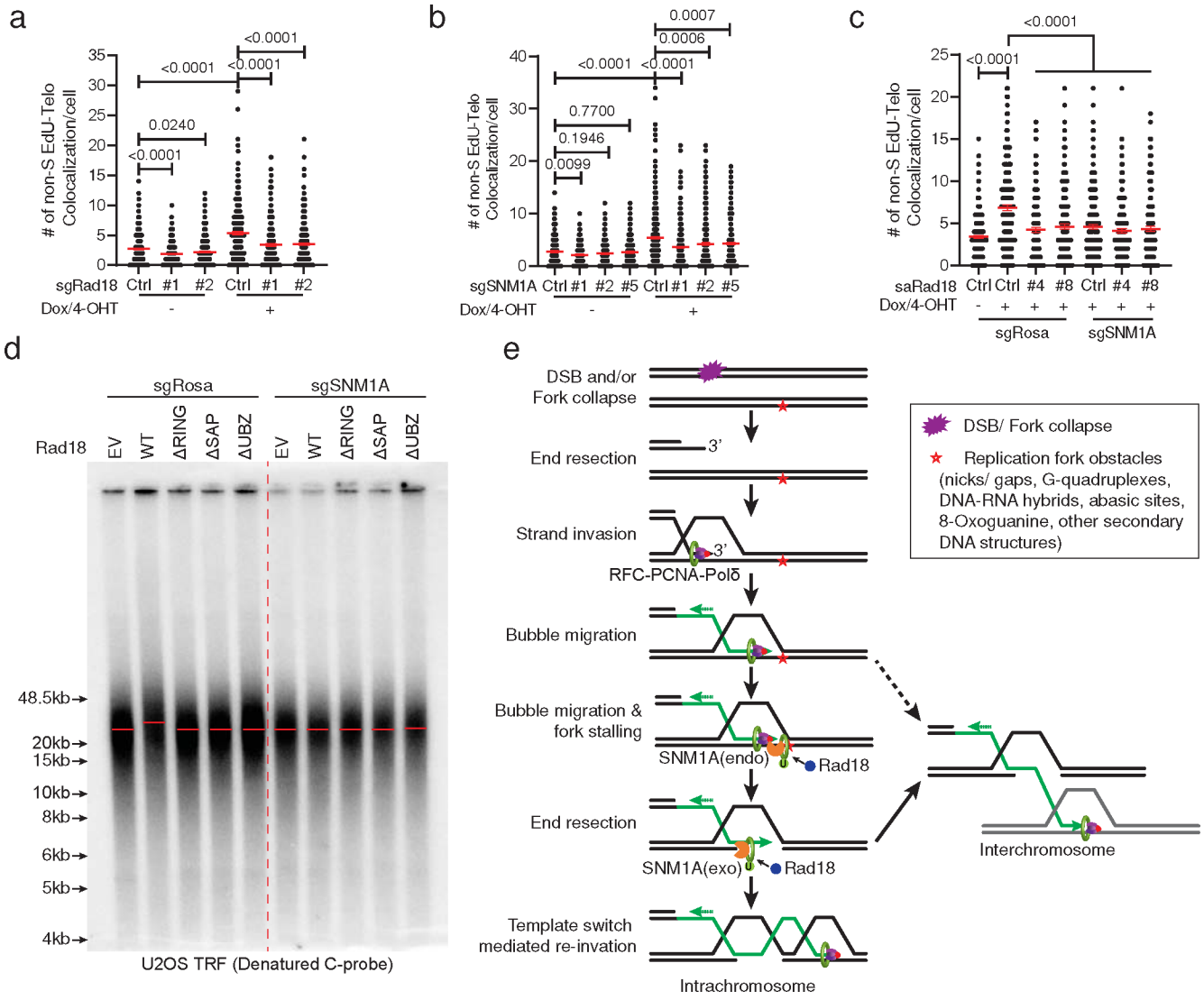

Figure 5. The RAD18-PCNA-Ub-SNM1A axis mediates template switch dependent lesion bypass to promote break induced replication.

a-c. Quantification of non-S EdU colocalization with telomeres in RAD18 **(a)** and SNM1A **(b)** single or double **(c)** knock out U2OS cells with or without TRF1-FokI induction for 2.5 hrs. Data represent the mean ± SEM of three independent experiments (n = 271, 311, 280, 283, 271, 249 in (**a**); n = 192, 222, 223, 184, 455, 436, 441, 443 in (**b**); n = 217, 186, 195, 205, 191, 213, 207 in (**c**) (left to right)). Statistical analyses were performed using an unpaired two-tailed student's *t*-test. *p* values are shown. **d.** Telomere Restriction Fragment (TRF) analysis of telomere length in U2OS cells that overexpress wild type RAD18 or the indicated mutants in the context of SNM1A proficient or knock out conditions. **e.** Model depicting PCNA-Pol δ encounters with lesions during break induced replication. This invokes DNA damage tolerance through RAD18 dependent PCNA-Ub interaction with SNM1A. The modified break induced replisome executes endonuclease mediated DNA nicking and 5'−3' exonuclease resection to promote template switch mediated lesion bypass. Template switching during BIR may also occur by dissociation of the 3'-end from its

original template and reinvasion into another template without end processing steps (right). This could occur in an SNM1A independent manner (dashed arrow).